PHOTOELECTRIC OBSERVATIONS OF THE ORION NEBULA AT SEVEN WAVELENGTHS

by

William Lawrence Reitmeyer

A Dissertation Submitted to the Faculty of the

DEPARTMENT OF ASTRONOMY

and of the

DEPARTMENT OF AERO-SPACE ENGINEERING

In Partial Fulfillment of the Requirements
for the Degree of

DOCTOR OF PHILOSOPHY

In the Graduate College

THE UNIVERSITY OF ARIZONA

1965

THE UNIVERSITY OF ARIZONA

GRADUATE COLLEGE

I hereby recommend that this dissertation prepared under my direction by William L. Reitmeyer

entitled Photoelectric Observations of the Orion Nebula at Seven Wavelengths

be accepted as fulfilling the dissertation requirement of the degree of Doctor of Philosophy

Hugh M. Johnson — 5/20/64
Dissertation Director — Date

After inspection of the dissertation, the following members of the Final Examination Committee concur in its approval and recommend its acceptance:*

Walter S. Fitch	9/24/64
Bruce T. Lyte	9/25/64
W. P. Bottomley	10/1/64
R. Anderson	10/27/64
E. K. Parks	10/27/64

*This approval and acceptance is contingent on the candidate's adequate performance and defense of this dissertation at the final oral examination. The inclusion of this sheet bound into the library copy of the dissertation is evidence of satisfactory performance at the final examination.

STATEMENT BY AUTHOR

This dissertation has been submitted in partial fulfillment of the requirements for an advanced degree at The University of Arizona and is deposited in the University Library to be made available to borrowers under rules of the Library.

Brief quotations from this dissertation are allowable without special permission, provided that accurate acknowledgment of source is made. Requests for permission for extended quotation from or reproduction of this manuscript in whole or in part may be granted by the head of the major department or the Dean of the Graduate College when in his judgment the proposed use of the material is in the interests of scholarship. In all other instances, however, permission must be obtained from the author.

SIGNED: William Lawrence Reitmeyer

TABLE OF CONTENTS

LIST OF TABLES

LIST OF ILLUSTRATIONS

ABSTRACT

Continuous slow motion intensity tracings in right ascension across the Orion Nebula were recorded at seven wavelengths, at each of six declinations. Data reductions of the intensity measures were made at two minute of arc intervals along each declination. The intensities of O^{++} at λ5007A, O^{+} at λ3727A, H_α and H_β, as well as the continuum intensities at λ3486A, λ4217A, and λ5100A are presented for eighty-eight points in the nebula. Electron temperature was determined at each point from the ratio of H_β to that of the Balmer continuum. The method employed to estimate the electron temperature requires a selection to be made of either Baker and Menzel's case A or of their case B (respectively transparent or opaque to Lyman line radiation). The average line of sight electron temperature varies from 3500° to 11700°K if case A is assumed and is less that 3500°K if case B is assumed. Accordingly, these results show a strong preference for case A, although uncertainties in the extrapolation for the intensity of the Balmer continuum prevent a conclusive statement as to the applicability of case A. The variation of the continuum intensity with wavelength, when compared with the resulting

electron temperature determined on the basis of case A, is in reasonable agreement with the expected variation if one-third of the electrons recombining or cascading to the second energy level enter the 2s level and return to the ground state with the emission of two-photon quanta. For an assumed model of eighteen minutes of arc radius, the root-mean-square electron density is found to vary from 370 to 30 electrons/cm^3. A section in the western part of the nebula, and another in the southeastern part, appear to be both deficient in O^{++} and to have higher electron temperatures than the neighboring areas. Both the temperature as determined here and the variation in the ratio of $N(O^+)/N(O^{++})$ indicate that the temperature is not a constant throughout the nebula, but rather depends on the position. This temperature dependence on the position does not appear to be a monotonically varying function of distance from the Trapezium.

CHAPTER I

INTRODUCTION

Among the more commonly observed celestial objects, particularily in the plane of our galaxy, there exists a group of luminous cloudlike areas known as bright diffuse nebulae. Members of this group are distinguished as being either of the line-emission type or of the reflection type. These nebulae are usually irregular in shape and have a typical representative diameter of 5 pc (Allen 1963). Although the nebulae are placed in one or the other category as their spectra show a predominance of emission lines or of continuous spectra characteristics, most show a mixture in that reflection nebulae often have emission features as do emission line nebulae have a continuous spectrum. In 1922, Hubble proposed an additional discriminant when he pointed out that the exciting star(s) was always B0 or earlier for emission line nebulae and of later type for reflection nebulae. A study of the spectrum of a nebula and of its exciting star allow the nebula to be placed into one of the two categories. Diffuse line-emission nebulae will be referred to as gaseous nebulae and it is to this category that the work presented here will be directed.

Gaseous nebulae represent dense regions of the interstellar medium and as such, the theory of these nebulae is a part of the theory of the interstellar medium. This medium is commonly viewed as an aggregate of individual clouds composed of gas and dust. When one or more of the clouds is associated with early-type stars, and the radiation from at least one of these stars causes the gas to become photoionized, a gaseous nebula exists. While not all early-type stars, thought to be younger than our galaxy, are found in gaseous nebulae, results found by Blaauw and Morgan (1953) indicate common origins for B stars — presumedly in nebulosity — and hence detailed investigations of gaseous nebulae are expected to afford information which will ultimately give an insight into the processes of star formation. Before this objective can be achieved, however, physical processes in a gaseous nebula must be well determined and observations of these nebulae offer the opportunity to test appropriate theories.

Historically, the theory of emission in nebulae was first given quantitative form in applications to planetary nebulae, and later extended to gaseous nebulae. Zanstra (1931a,1931b) proposed a theory of ionization and recombination in nebulae based on the assumption that ultraviolet radiation short of the Lyman limit (912A) is completely

absorbed in the interior of the nebulae. One supposes a nebula to be composed almost entirely of hydrogen, with essentially all neutral hydrogen atoms in their lowest level; the star to radiate as a black body; and the nebula to absorb all radiation from the star at wavelengths less than the Lyman limit. One further assumes all ionizations to take place from the ground level; recombinations to take place to any level; and the electrons to cascade downward from excited levels at rates determined only by the Einstein transition probabilities. This ionization and subsequent recombination and cascade is taken as the primary mechanism of excitation.

If the free electron, following ionization, recombines to the ground level, a photon identical to the original ionizing photon is emitted, leaving it free, in turn, to ionize another hydrogen atom. Recombination to the second level with emission of a photon of the Balmer continuum is followed by emission of a Lyα photon in the transition to the ground level. Recombination to the third level is accomplished with the emission of a photon of the Paschen continuum. The subsequent transition to the ground level may be direct, with the emission of a Lyβ photon, or it may cascade through the second level with the emission of both Hα and a Lyα photon. The possible number of photons of different energies evidently increases as recombination is to higher and higher levels. It is assumed

that all photons of the Balmer and higher series, as well as their continuum emission, are not reabsorbed in the nebula, and that the Lyα photons are simply scattered (neglecting for the moment the two-photon process) and ultimately escape the nebula. In a nebula composed primarily of hydrogen, this method then allows an estimate to be made of the temperature of the exciting star. One measures the energy of the star at an accessible wavelength and from the measured strength of the Balmer lines and visual continuum of the nebula calculates the energy radiated by the star short of the Lyman limit. These two energies may then be fitted to a black body radiation curve, from which the temperature of the exciting star is determined. This method has been applied extensively to temperature determinations of the exciting stars of planetary nebulae.

Another approach to the interpretation of nebular spectra was formalized by Menzel and Baker (1937). They assumed a nebula in which nc account is made of the Lyman line radiation from the star, and all radiation from recombinations within the nebula leaves freely without absorption. This model is designated case A. Case B modifies case A to account for the nebular radiation field, but not that of the star, by assuming that no Lyman line radiation other than Lyman alpha escapes the nebula. Then if the nebula is transparent to the Lyman line

radiation, all Lyman series photons will leave the nebula and case A will be applicable. On the other hand, if the nebula is not optically thin to the Lyman line radiation, radiation from Lyβ and higher series members will ultimately be degraded into a Balmer photon and a Lyα photon, both of which will escape the nebula. If this latter mechanism, case B, is operative within the nebula, there will be a strengthening of the observable Balmer lines and a steepening of the Balmer decrement. In both cases the primary method of excitation is ionization followed by recombination and cascade. It is this approach that is most often applied to gaseous nebulae and that will be used here.

Menzel (1937) pointed out that in a gaseous nebula, the only part of the gas likely to approach thermodynamic equilibrium would be the free electrons, which will essentially have a Maxwellian distribution defined by the kinetic electron temperature, T_e. A considerable simplification of the equations appropriate to these models will result from all processes being referred to electron captures. The dissociation formula, which allows the number of atoms in level n to be calculated as a function of the number of ions, N_i, the electron temperature, the number of electrons, N_e, and known atomic parameters, will in this application also include a b_n term which is a measure of the departure from thermodynamic

equilibrium. The b_n terms, originally calculated by Baker and Menzel (1938), have been recalculated by Seaton (1959) and are given as functions of the electron temperature for case A and case B. Electron temperature has commonly been found from the ratio of the [OIII] lines (Menzel, Aller and Hebb 1941) and the density then found from the expressions for the intensity of one of the Balmer lines or continuum. From the line intensities near the series limit in the Orion Nebula, Greenstein (1946) estimated the electron temperature to be 6500°K, based on Baker and Menzel's (1938) case B, in the central portion of the nebula. Using the b_4 as calculated by Seaton (1959), this corresponds to 4800°K for case B and 17000°K for case A. From the energy distribution to the red side of the Balmer limit, Greenstein deduces a temperature of approximately 12000°K.

If the temperature and density are known, the amount of O^+ and O^{++} may be determined. Since the oxygen may be assumed to be either O^+ or O^{++}, determination of the abundance of these in turn allows the total abundance of oxygen to be estimated. The strength of O^+ may be determined from the intensity measures of the doublet at λ3727A, the strength of O^{++} from the intensity of the N1 line at λ5007A. Of these two collisionally excited lines, the O^{++} is the more effective cooling agent. Accordingly, with the total amount of oxygen

held constant, the temperature should vary inversely as the amount of O^{++}(Burbidge, Gould and Pottasch 1963).

The observable continuum in nebulae may contain, in addition to the bound-free transitions already mentioned, free-free transitions, two-photon emission, and light scattered by dust. Hall (1951) has shown that the light in the Orion Nebula is slightly polarized, indicating some scattering, but it is generally held (Dufay 1957) that scattering plays only an accessory role in most nebulae. Greenstein (1946) suggests that this reflection continuum has an intensity of between 10 and 20 per cent of the Balmer continuous emission in the Orion Nebula. Page (1942) has studied the distribution of the visual continuum intensity (to the red side of the Balmer continuum) and found the intensity in planetary nebulae to be essentially independent of wavelength in the range from λ3900A to λ5000A. Free-free transitions may contribute to the intensity of the visual continuum at all wavelengths. Greenstein and Page (1951) estimate that only 5 per cent of the intensity observed at λ3900A can be accounted for by free-free transitions. They also determined that the amount of H^- present in gaseous nebulae is so small that the continuum cannot be accounted for from the process of H^- formation. Spitzer and Greenstein (1951) have considered the two-photon process in detail. They have concluded that approximately 32 per cent of the electron

captures to the second level will go to the metastable 2s level, from which only two photons may be emitted, the sum of their energies equalling the energy of the Lyα photon. The amount of two-photon emission can be enhanced by collison of a free electron with an excited hydrogen atom, in the 2p level, inducing a transition to the 2s level, followed by two-photon emission. The low probability of the collisional transition may be offset by the large number of times Lyα radiation is thought to be scattered in a nebula. The two-photon emission increases with frequency and hence, will cause the color of the continuum to become more blue.

This work proposes to measure the intensities of selected emission lines and portions of the visual and Balmer continuum at many points over the observable area of the Orion Nebula. Because of its large apparent size and its availability to observers in the Northern Hemisphere, the Orion Nebula is well suited to such observations. A spectrographic survey of this nebula has been made by Osterbrock and Flather (1959), a radio survey at 3.75 cm wavelength has been made by Menon (1961), and Boyce (1963) has observed the bright portion of the nebula with a spectrophotometer to determine relative strengths of some of the Balmer lines. The Orion Nebula is commonly held to have an electron temperature of approximately 10000°K, which is usually assumed constant through the nebula.

It is thought to have considerable dust mixed with gas, to be optically thick, and well represented with Baker and Menzel's (1938) case B. Excitation and illumination have been ascribed primarily to the O6 star of the Trapezium group (θ^1 Ori), of spectral types O6-B3. The continuous spectrum is strong and it is considered possible that two-photon emission makes a sizeable contribution to this continuum. This work is intended to make observational data, for many points in the Orion Nebula, available to interested investigators in this field, as well as to offer the possibility of testing some of the basic assumptions about the radiation field, electron temperature and its distribution, and oxygen abundance commonly used in models proposed for the Orion Nebula.

CHAPTER II

EQUIPMENT

The observations were made at the Steward Observatory of the University of Arizona using a photoelectric photometer on the 36 inch telescope. This reflecting telescope is equipped with suitable optics to allow observations to be made at the Newtonian, Cassegrain, or coudé positions, respectively having focal ratios of f/5, f/15, and f/36.

A photoelectric photometer for use at the Newtonian position, with all necessary support equipment, i.e. high voltage supply, amplifier with gain graduated in one-half magnitude steps, Leeds and Northrup recorder, etc., was available at the time this project was undertaken. Consideration however, had to be given to optimizing the focal ratio to best suit these particular observations. An increase in focal ratio to f/15 offered several advantages. A larger focal ratio than that of the Newtonian position would allow the light rays passing through the filters to be more nearly parallel, as is desired when using interference filters. Increased focal ratio would be accompanied by a greater scale and permit accurate positioning to be done with considerably greater facility. The Cassegrain position, with focal ratio of f/15, was selected as

being the most desirable for these observations.

A new photocell holder had to be designed for use at the Cassegrain position. The following considerations governed this design. The new holder had to accomodate, in addition to the photocell, at least seven filters, one inch square or one inch in diameter, and approximately one-half inch thick. It was necessary to be able to change the filters from one to the other with only a momentary loss of observation time. They had to be so placed in the light path that the incident beam totally passed through the filter, while at the same time utilizing a sufficiently large portion of the filter area that any irregularities in the filter would be minimized. The photocell was to be enclosed so that it could be refrigerated and thereby reduce the dark current and noise level to as low a value as possible. The existing Newtonian photometer was so constructed that the photocell holder could be easily removed. The rest of the photometer, containing the diaphragm, the field lens, the gain control panel, and the adapter to the telescope could all be used at the Cassegrain position. The new holder was so designed that it was interchangeable with the old and the photometer could be quickly adapted to either position. For maximum utility, the recepticle for the photocell in the new holder was designed to have the same attachments as in the old so that the photocell and connections could be used in either holder.

The overall geometry of the photocell holder was dictated by the requirements of the optical system. The filters were located in the light path so that the image spot size on the filter would be one-half inch. The Fabry lens was placed directly behind the filters, its purpose being to image the objective on the photocathode. For an RCA IP21 photocell, a 3/16 inch diameter image allowed all the light to fall on the photocathode, yet be only slightly less than the minimum dimension of the photocathode itself. The diameter of the diaphragm was chosen to be 4mm, corresponding to one minute of arc. This offered an acceptable compromise of good resolution and measurable light intensity for diffuse nebulae. Knowing these quantities, the position of the Fabry lens and the photocell in the light path was specified. The Fabry lens was made of fused quartz and had a focal length of 2.75 inches at λ4900A.

The cold box of the photocell holder consisted of a copper box, 3 inches square and 2.5 inches deep, to the outside bottom of which was silver soldered a length of 2 inch o.d. copper pipe and into which the photocell was to be inserted. This was insulated from the outside shell of the holder by Styrofoam. Polyethylene tubing separated the photocell encasement from the Fabry lens holder and from the outside shell. Dry ice was placed into the cold box by opening the hinged top, removing a one inch thick layer of Styrofoam, and inserting

it into the copper box. By refrigerating the photocell, the dark current was reduced — at full gain — from 75 per cent of full scale deflection on the recorder to less than 7 per cent, and the noise from ± 5 per cent to less than ± 0.5 per cent. The photocell required twenty minutes to come to operating temperature and showed no variation of dark current or noise level for an eight hour period after having come to operating temperature.

The filter tray was originally made of aluminum, as was the entire shell of the photometer. It was found, in trials of the equipment, that the aluminum to aluminum contact of the sliding surfaces tended to produce dust which collected on the filters. The aluminum tray was replaced with one made of wood and held away from the aluminum case by small round head brass tacks. Each of the filters could be placed in the light path by a push-pull motion of a rod connected to the tray and extending outside the case, a detent having been built in to assure proper positioning of each filter. Figure 2.1 is a cut-away sketch of the partially assembled photometer.

The filter characteristics were determined from the response curves obtained with the Kitt Peak National Observatory Cary recording spectrophotometer. Response curves were obtained in the Fall of 1961 and the Summer of 1962. The only filter that showed an appreciable variation over this time

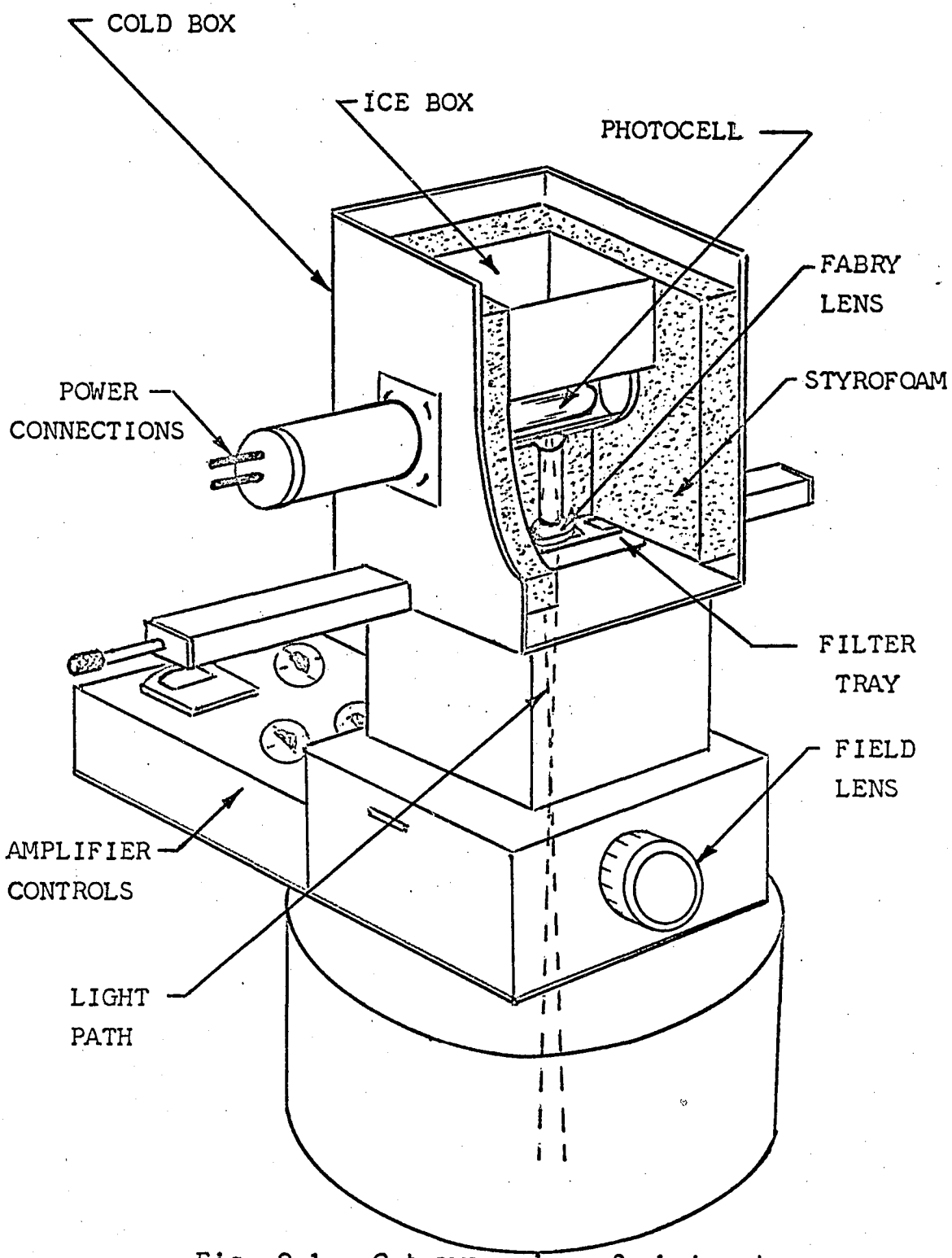

Fig. 2.1 - Cut-away view of photometer

span was the λ5003A filter. A detailed discussion of this variation is to be found in a later chapter. The peak positions (in the case of the λ5100A and of the λ3486A filters, the word peak should be interpreted as effective wavelength or mean position at which one-half the equivalent width lies to either side), the principal features, the maximum transmissions, the one-half band widths, the equivalent widths, and the wavelengths at one per cent transmission of each filter are tabulated in Table 2.1. The first six filters are interference filters and the seventh is a glass filter. The response curves of these filters are given in Figures 2.2 - 2.8.

The amplifier gain controls consisted of both a fine and a coarse gain setting. The coarse gain ranged from 1 to 4 in approximate two and one-half magnitude steps, while the fine gain ranged through two and one-half magnitudes in precise one-half magnitude steps. The coarse gain was calibrated by obtaining a recorded percentage response through the instrument, to an imput signal, at different gains.

The slow motion drive rate of the telescope was determined by driving with the slow motion controls between stars of common declination and known right ascension in the Orion Nebula. Several of these pairs were contained in the right ascension tracings made through the nebula. The drive rate was found to be a constant 0.771 minutes of arc per minute of time

TABLE 2.1

FILTER CHARACTERISTICS

Peak Position (A)	Principal Features	Maximum Transmission (%)	Band Width at 1/2 maximum Transmission (A)	Equivalent Width (A)	Wavelength at 1% Transmission (A)
λ6564	H_α	40.4	6.8	3.3	λ6550 - λ6582
λ5100	O^{++}	78.8	194.2	160.1	λ4910 - λ5299
λ5003	O^{++}	55.5	15.8	12.4	λ4952 - λ5051
λ4857	H_β	59.6	12.5	10.2	λ4818 - λ4900
λ4217		45.5	41.1	19.8	λ4163 - λ4277
λ3722	O^+	44.0	28.4	18.1	λ3651 - λ3803
λ3486		43.0	68.9	43.7	λ3323 - λ3708

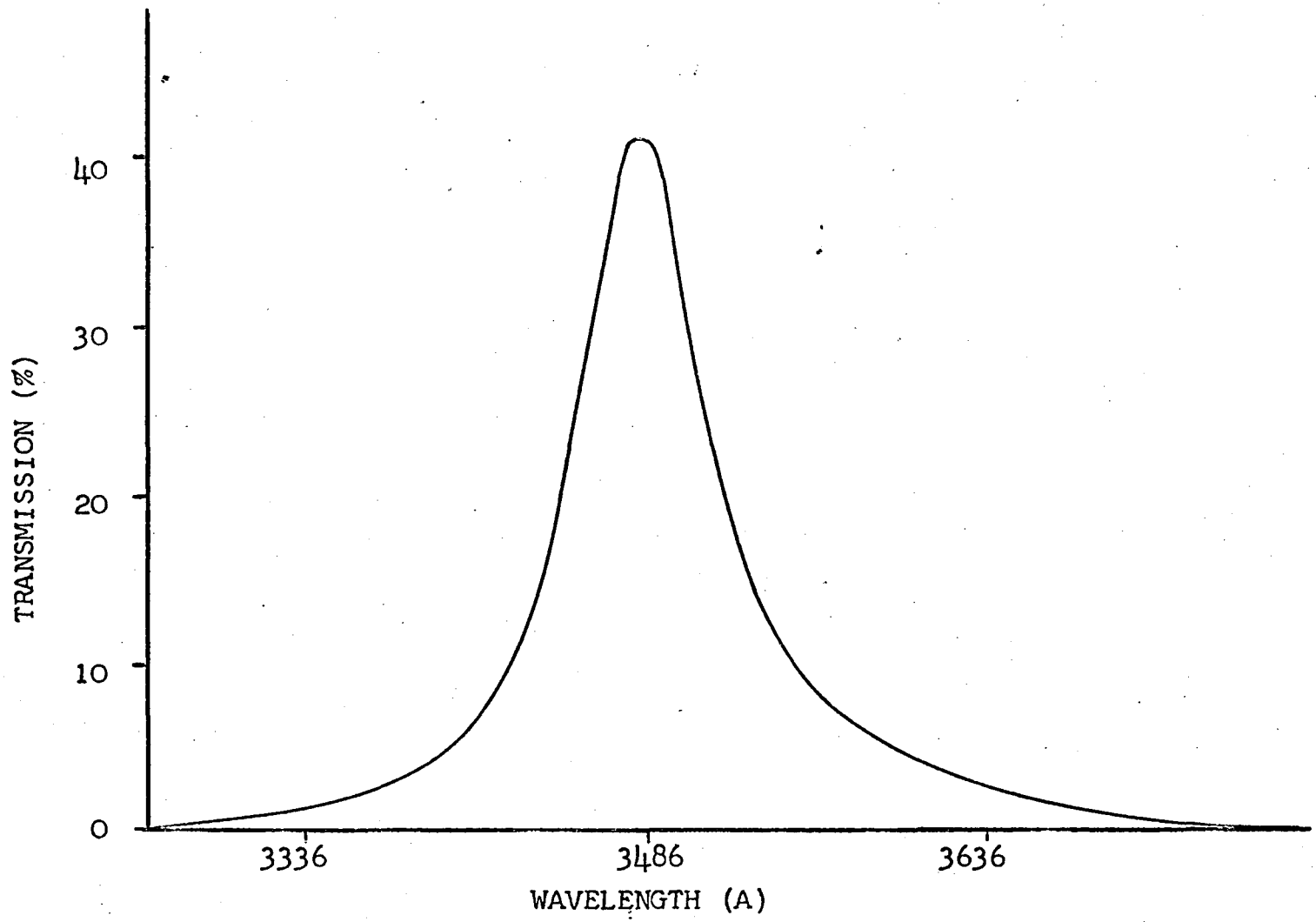

Fig. 2.2 - Transmission curve of the λ3486A filter.

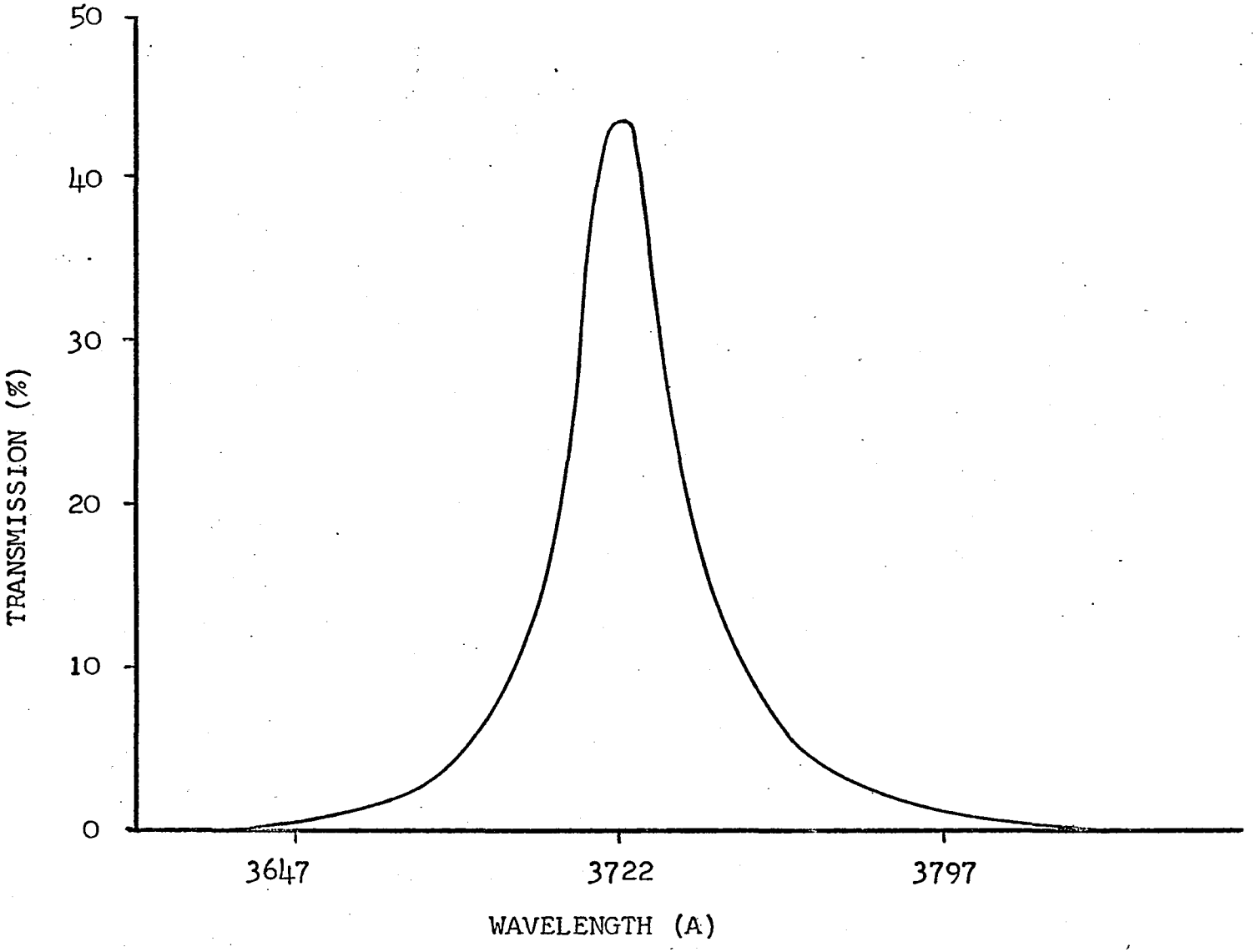

Fig. 2.3 - Transmission curve of the λ3722A filter.

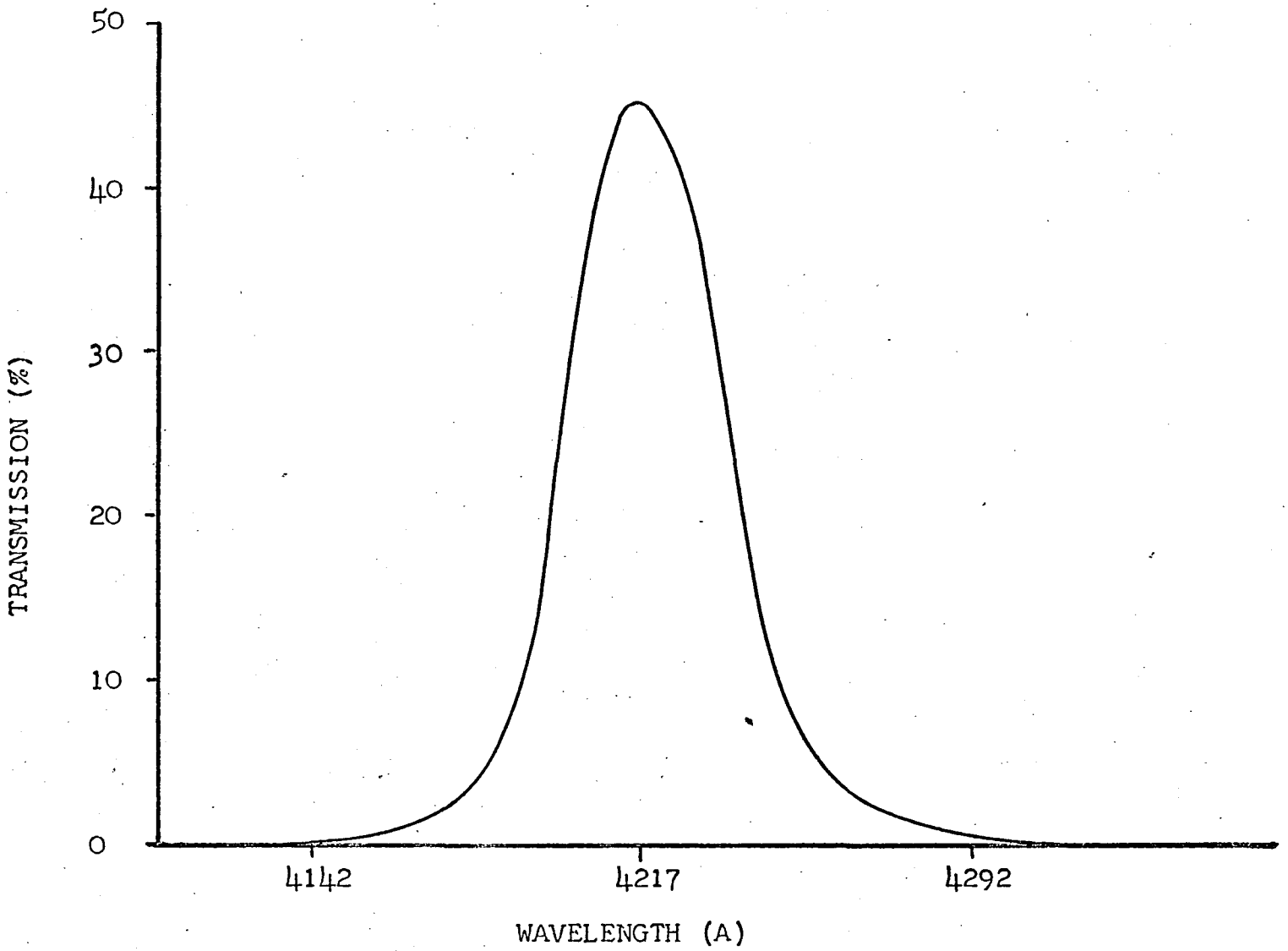

Fig. 2.4 - Transmission curve of the λ4217A filter.

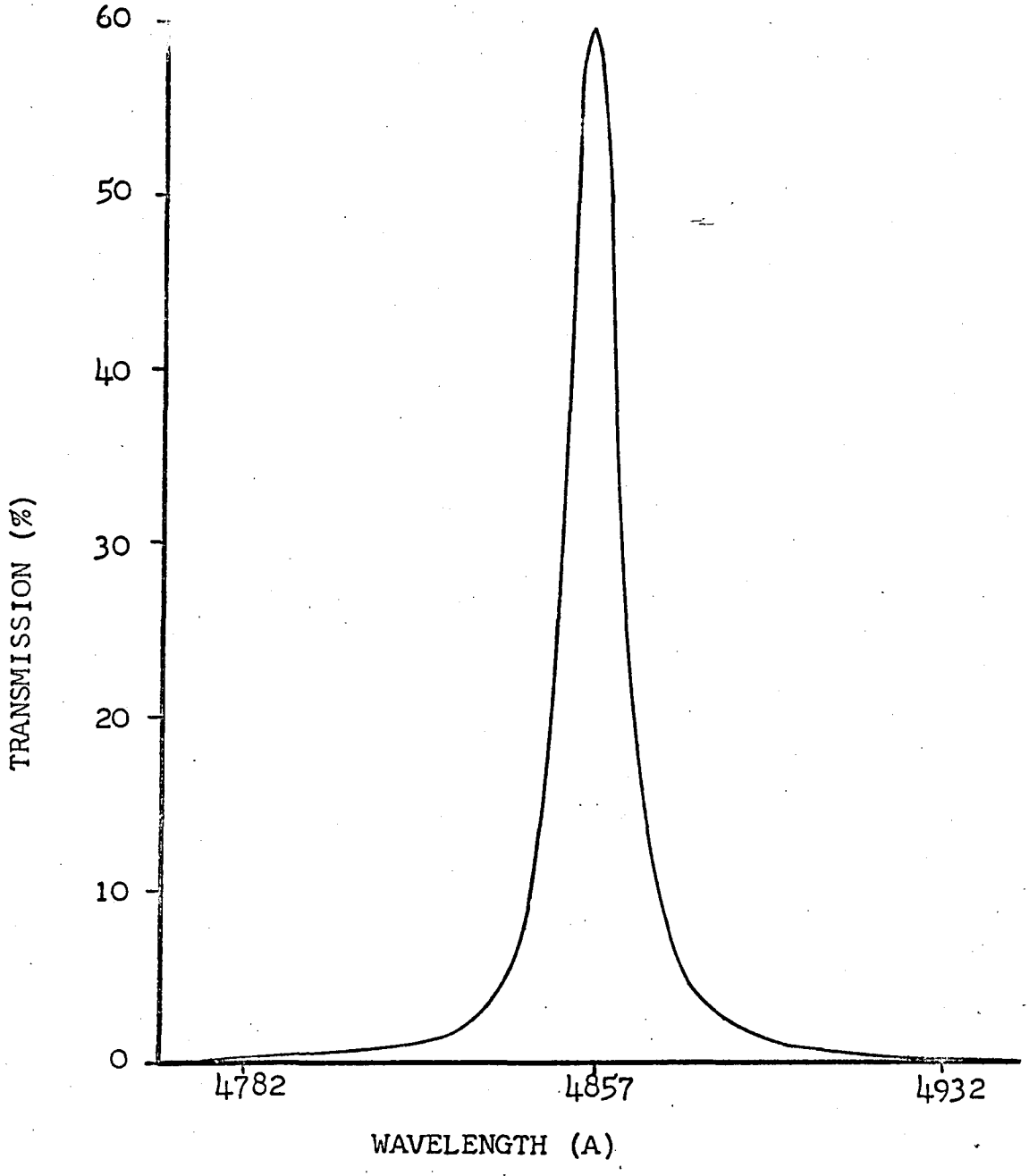

Fig. 2.5 - Transmission curve of the λ4857A filter.

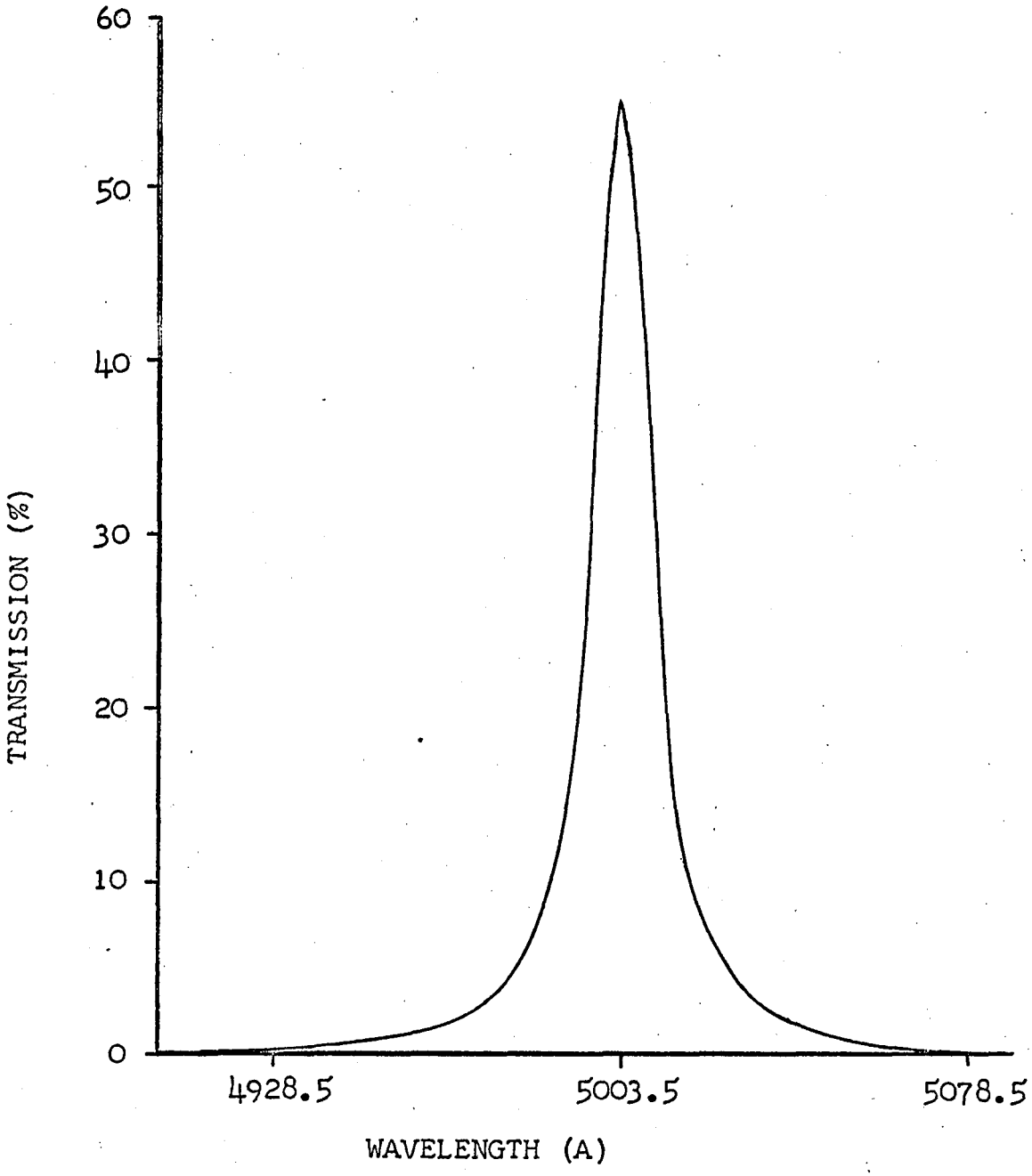

Fig. 2.6 - Transmission curve of the λ5003A filter.

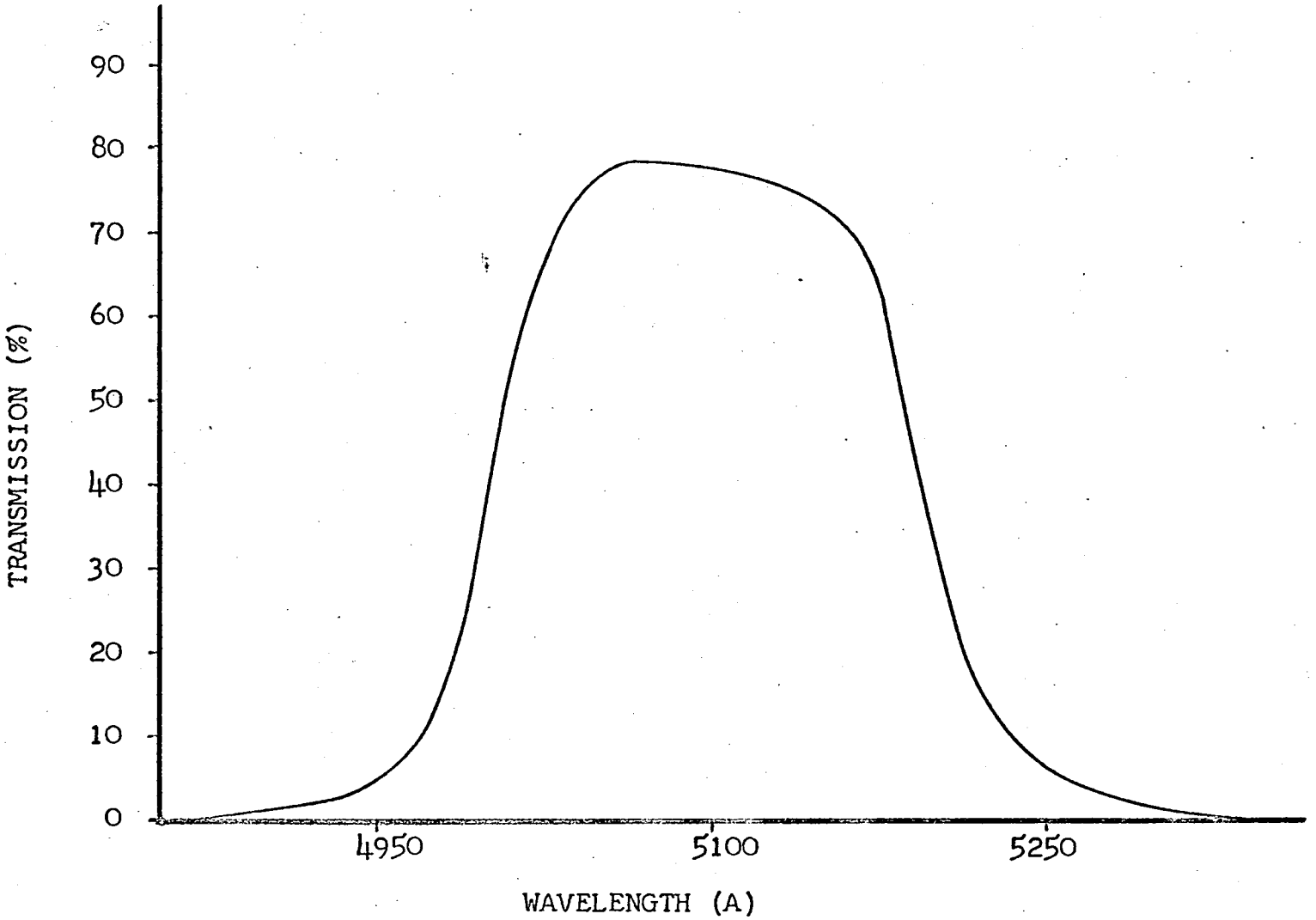

Fig. 2.7 - Transmission curve of the λ5100A filter.

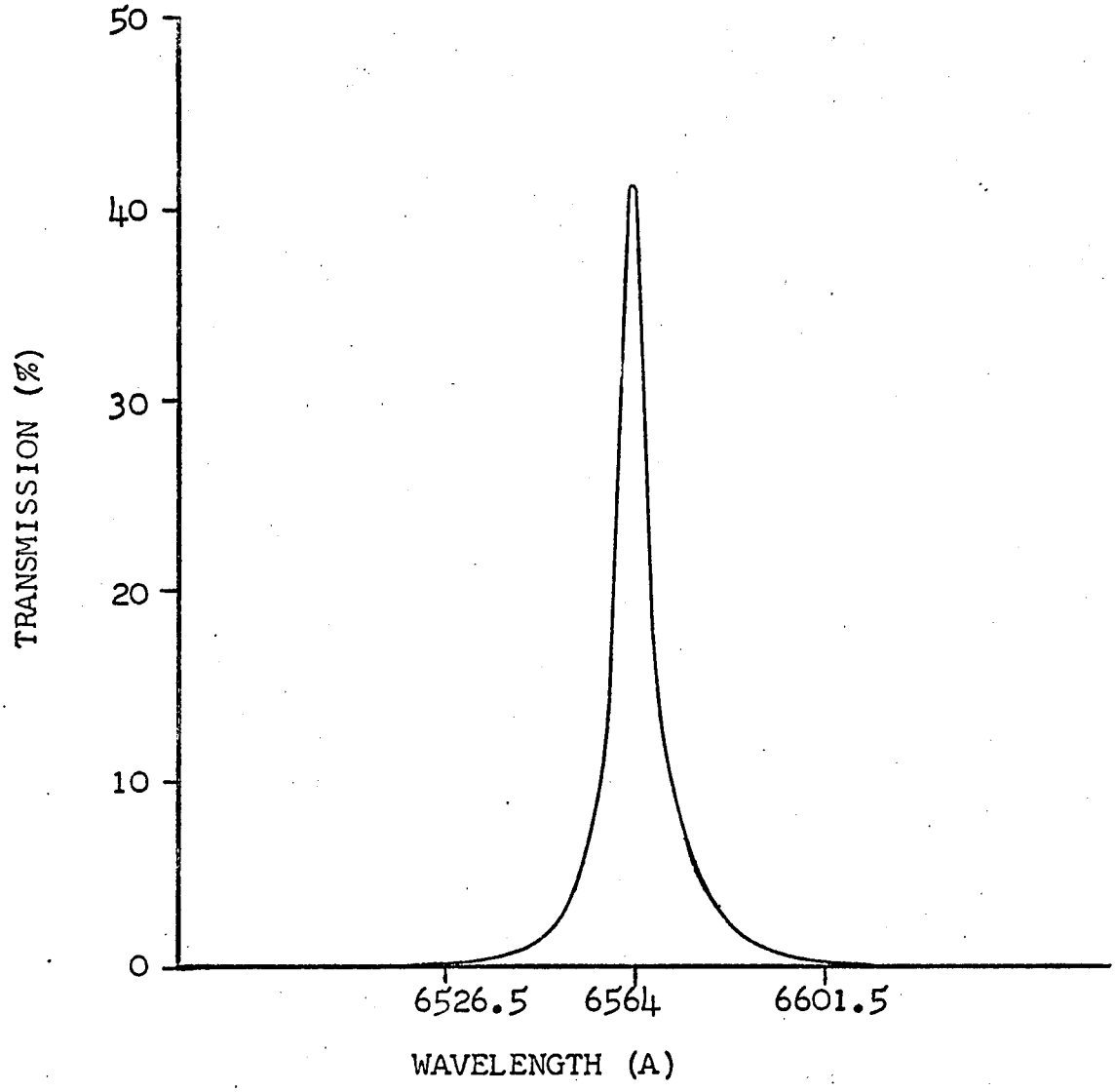

Fig. 2.8 - Transmission curve of the λ6564A filter.

for the range of hour angle of ± 2 hours, to which these observations were restricted. Accompanying this drive rate was a drift in the direction of decreasing declination of 0.521 minutes of arc per hour. Similar evaluations were made for the slow motion drive in declination and the rate was found to be 0.617 minutes of arc per minute of time, with a drift in the direction of increasing right ascension of 0.521 minutes of arc per hour.

CHAPTER III

REDUCTIONS OF OBSERVATIONAL DATA

1. Extinction

Observations of the Orion Nebula were made on nineteen nights, from January 19, 1962 to March 17, 1962. On each of these nights, both before and after observations of the nebula, intensity measures through all filters were made of νOri and δTau, recorded with the nebular observations, and used to compute the correction for extinction in the following manner: For observations taken at any one time, $m_\lambda = m'_\lambda - K_\lambda X$, where:

m_λ is the magnitude, at a particular λ, corrected for extinction.

m'_λ is the magnitude, at λ, recorded and uncorrected for extinction.

K_λ is the extinction coefficient in magnitudes.

X is the air mass along the line of sight, in units of the zenith air mass taken as one.

In these observations, since X does not exceed two air masses, the customary assumption that $X = \sec Z$ is made, where Z is the angle from zenith to the observed object.

Letting $C_{ij} = m_i - m_j$, the extinction coefficients in

colors may be determined such that $C_{ij} = C_{ij}' - (K_i - K_j)X$, or $C_{ij} = C_{ij}' - k_{ij}X$ where:

C_{ij} is the color corrected for extinction;

C_{ij}' is the color uncorrected for extinction;

k_{ij} is the color extinction coefficient;

X is the common air mass.

Since C_{ij}' and X vary from observation to observation, and with k_{ij}, from night to night, $C_{ij} = C_{ijpn}' - k_{ijn}X_p$, where the indices i and j indicate wavelengths, n indicates a particular night, and p a particular observation on any n. It is thereby assumed that C_{ij} for υOri and for δTau — taken as standard stars for these observations — remains unchanged. In other words, the color of a standard star, when corrected for extinction, is an invariant.

Eight of the nineteen nights were chosen as typical and with thirty-two readings, a least square solution yielded C_{ij} for the standard stars, as well as k_{ijn} for these eight nights. Using C_{ij}, X_p, and C_{ij}', k_{ijn} for each of the remaining eleven nights was determined. This solution was made for two colors, namely $C_{ij} = C_1 = m_{\lambda 3486} - m_{\lambda 5100}$ and $C_2 = m_{\lambda 3486} - m_{\lambda 4217}$. There existed an excellent correlation between the k for C_1 and the k for C_2 such that $(k_1/k_2)_n = 1.58 \pm 0.0027$ where the deviation is given in terms of mean error of the mean.

The magnitude extinction coefficient for λ5100A, $K_{\lambda 5100}$, may then be determined. In the most general form,

$$m_\lambda = m_\lambda' - K_\lambda(\sec Z) + \alpha t - Z.P. \qquad (3.1)$$

where α is a linear time correction for instrument sensitivity in magnitudes per hour and Z.P. is the zero point or night correction, in magnitudes, to one night chosen as a base night. For the standard stars, the difference of an observation on each of them may be written as:

$$m_\upsilon - m_\delta = m_\upsilon' - m_\delta' - k_\lambda(\sec Z_\upsilon - \sec Z_\delta) + \alpha(t_\upsilon - t_\delta) - (Z.P._\upsilon - Z.P._\delta). \qquad (3.2)$$

For observations made on the same night, $(Z.P._\upsilon - Z.P._\delta) = 0$. For observations made at the same time, $(t_\upsilon - t_\delta) = 0$. For observations made at the same X, $(\sec Z_\upsilon - \sec Z_\delta) = 0$. All of these conditions are satisfied for four sets of observations yielding: $0.485 \leqq (m_\upsilon - m_\delta) \leqq 0.503$, or $(\overline{m_\upsilon - m_\delta}) = 0.495$.

For two other sets of observations, the first two conditions are satisfied while $(\sec Z_\upsilon - \sec Z_\delta) > 1/3$ air mass. From these observations, knowing $(\overline{m_\upsilon - m_\delta})$, extinction coefficients are found for these nights. These in turn are compared to k_1 for the same nights with the result that $(K_{\lambda 5100}/k_1)_n = 0.372$. It is then assumed that $(K_{\lambda 5100})_n = 0.372\ k_{1n}$ and $K_{\lambda 5100}$ is found for each night.

Using k_{1n}, k_{2n}, and $K_{\lambda 5100}$, a K versus λ curve is constructed for each night and the K for each λ found. The

zero point correction for each night, relative to one night taken as a base, may be determined from the intial reading for that night. The α for each night may be found from the conditions that the initial and final magnitudes must agree and that $(m_{\upsilon} - m_{\delta})_n = \overline{(m_{\upsilon} - m_{\delta})}$. Figure 3.1 shows a plot of Allen's (1963) K versus λ for the range of λ of interest, accompanied by the extreme values of the observations described here.

For four nights, with large air mass and α known (found to be independent of λ), $K_{\lambda 6564} = 0.114$. This value is then taken independent of the night since $K_{\lambda 6564}$ is small, the instrument sensitivity is poor at this λ, and on these four nights, $K_{\lambda 6564} = 0.114 \pm < 0.01$.

The α, the Z.P., and the K_{λ} for the λ of interest are tabulated in Table 3.1.

An instrument magnitude for a standard star, m_{λ}, may then be determined from $m_{\lambda} = m'_{\lambda} - K_{\lambda}(\sec Z) + \alpha t - Z.P.$ For υOri the results are given in table 3.2.

2. Planetaries

In the course of rechecking the calibration curves of the filters, it was found that the peak of the λ5003A filter had shifted 6A over a period of one year. A shift of this magnitude can be critical on a filter of so narrow a 1/2 band width (15.8A). A straight line variation of the peak position

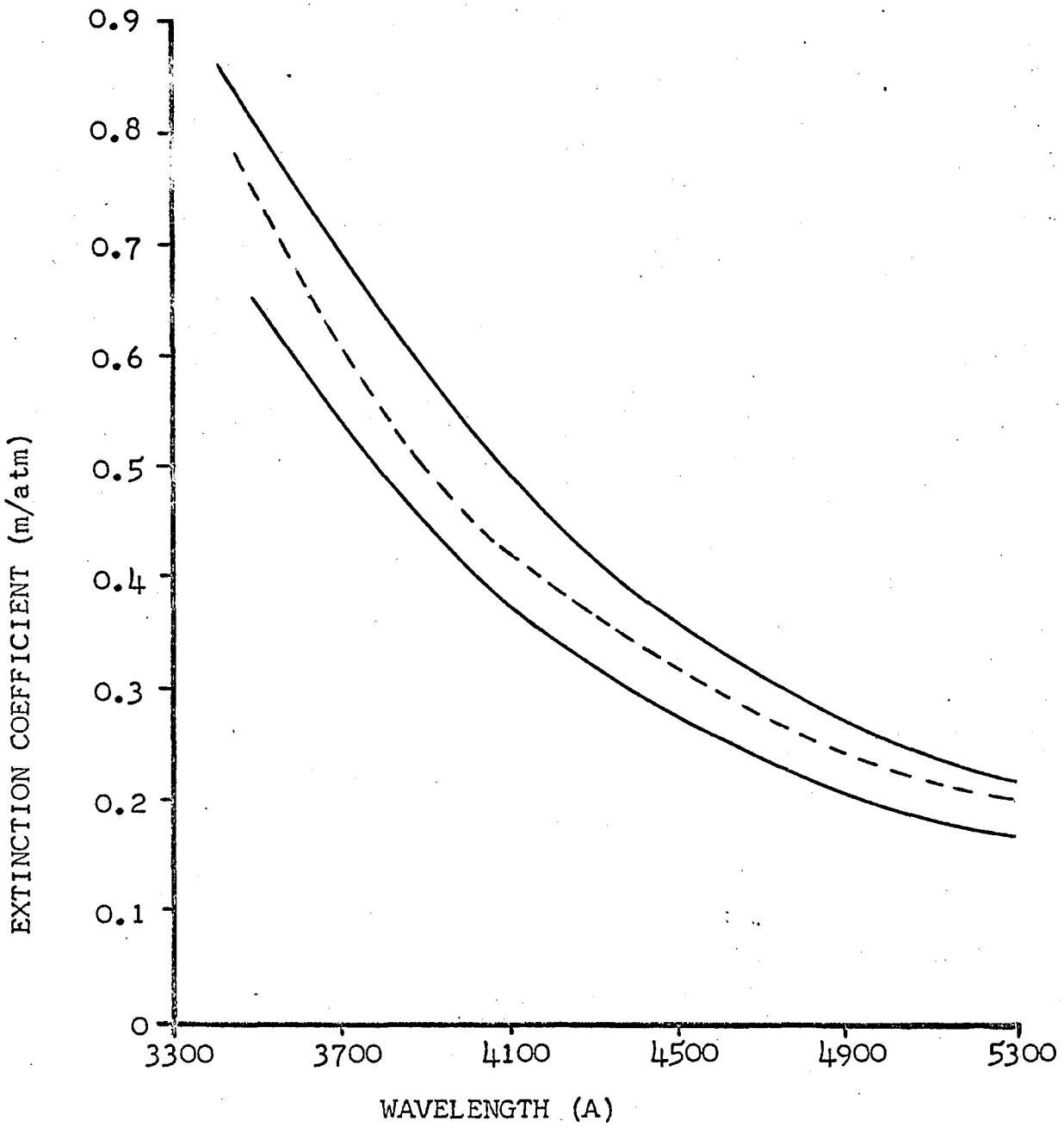

Fig. 3.1 - Comparison of the extreme values of the extinction coefficient used in these data reductions (solid line) with a mean value of this coefficient (dashed line) suggested by Allen (1963).

TABLE 3.1

DATA FOR THE EXTINCTION CALCULATIONS

Night	Z.P. (mag)	α (mag/hr)	$K_{\lambda 5100}$ (mag)	$K_{\lambda 5003}$ (mag)	$K_{\lambda 4857}$ (mag)	$K_{\lambda 4217}$ (mag)	$K_{\lambda 3722}$ (mag)	$K_{\lambda 3486}$ (mag)
1	0.126	+0.011	0.182	0.195	0.220	0.361	0.548	0.670
2	0.071	+0.012	0.184	0.197	0.222	0.361	0.553	0.677
3	0.023	+0.006	0.179	0.190	0.214	0.351	0.540	0.660
4	0.000	-0.004	0.183	0.193	0.215	0.357	0.554	0.674
5	0.063	-0.001	0.183	0.194	0.217	0.366	0.558	0.675
6	0.062	-0.003	0.193	0.204	0.231	0.389	0.590	0.711
7	0.080	-0.011	0.223	0.238	0.268	0.452	0.679	0.822
8	0.094	-0.012	0.222	0.235	0.264	0.443	0.676	0.819
9	0.070	-0.006	0.177	0.187	0.209	0.341	0.535	0.654
10	0.015	-0.006	0.180	0.193	0.217	0.352	0.546	0.664
11	0.054	+0.015	0.183	0.197	0.224	0.372	0.565	0.689
12	0.044	+0.009	0.193	0.206	0.232	0.387	0.582	0.712
13	0.072	+0.013	0.182	0.194	0.216	0.361	0.552	0.670
14	0.017	+0.008	0.193	0.204	0.229	0.383	0.583	0.711
15	0.021	-0.005	0.199	0.212	0.239	0.401	0.610	0.735
16	0.066	+0.013	0.197	0.208	0.235	0.391	0.601	0.727
17	0.137	+0.020	0.203	0.215	0.245	0.407	0.622	0.748
18	0.110	+0.015	0.205	0.217	0.245	0.406	0.622	0.747
19	0.053	0.000	0.195	0.207	0.233	0.389	0.589	0.719

TABLE 3.2

DATA FOR STANDARD STAR ν ORI

Filter	Flux/A	W x Flux/A	m	m'	S
λ6564	2.37×10^{-11}	7.83×10^{-11}	11.020	7.287	3.2
λ5100	6.90×10^{-11}	1.11×10^{-8}	2.168	1.939	81.0
λ5003	7.42×10^{-11}	9.20×10^{-10}	4.781	4.637	87.6
λ4857	8.29×10^{-11}	8.46×10^{-10}	4.729	4.729	100.0
λ4217	1.36×10^{-10}	2.69×10^{-9}	3.537	3.471	94.2
λ3722	1.95×10^{-10}	3.50×10^{-9}	3.284	3.177	90.6
λ3486	2.26×10^{-10}	9.88×10^{-9}	2.357	2.060	76.1

was assumed, but an independent check on the validity of this assumption is to be desired. In addition, it is necessary to eliminate the variation of the intensity with λ of the total instrument sensitivity, to effectively compare intensities at different λ. This can be accomplished by adopting a flux distribution of σOri as given by Code (1960). Code's system, however, compares continuum flux and it is necessary to have an estimate of the depression of the continuum in σOri through the H_β filter.

Both the above mentioned problems, namely the verification of the λ5003A filter peak position and the determination of the amount the H_β filter is to be corrected to give pure continuum, are amenable to solution with observations made on selected planetary nebulae that were also observed by Capriotti and Daub (1960).

In addition to observations of Planetary Nebulae NGC 6210 and NGC 6543, two of Code's standard stars, η UMa and α Lyr were observed on the same night. Mean extinction coefficients were assumed and the zero point and α correction determined, bringing the planetary observations to the same instrument magnitudes as those used for the Orion observations.

An estimate of the continuum strength, of both planetaries, to be expected in the λ5100A range was made in the following manner. The intensity of the continuum, summed from

λ4400A to λ5000A was put equal to the intensity of Hδ (Aller 1956). The intensity of H_δ was set equal to 1/4 the intensity of H_β (Berman 1936). The continuum strength per angstrom was assumed constant over this wavelength interval and adopted as the continuum strength at λ5003A and λ5100A. From Capriotti and Daub's work (1960), the ratio of the flux of the N1 line to that of H_β was made, thereby allowing an estimate of the continuum strength as a fractional part of the N1 line. For both filters, the total flux received through the filter was a percentage transmission of the N1 line plus continuum. From the difference of the instrument magnitudes through each filter the ratio of fluxes was determined, leading to a relation between the percentage transmission of the N1 line for the two filters. Since two planetaries were observed, two relations were found. For NGC 6210, the contribution of the continuum through the λ5003A filter was in this manner estimated to be 0.5 per cent and for NGC 6543, 1.0 per cent.

The radial velocities of these nebulae were given by Campbell and Moore (1918). By the method of Herrick (1935), the velocities were corrected to the earth on the night observed. The exact λ of the N1 line was found to be λ5006.8A for NGC 6210 and λ5006.0A for NGC 6543. Using the observed magnitudes of the standard star and planetary nebula, the flux of each as given by Capriotti and Daub (1960), and the

equivalent width of the filter, the percentage transmission through the λ5003A filter was determined from:

$$\text{Log } \frac{1}{\%T} = \frac{(m^{nb} - m^{*})}{2.5} + \text{Log } F_{N1} - \text{Log } F_{ct^{*}/A} - \text{Log } W_{\lambda 5003}. \quad (3.3)$$

From the previously found relation between the percentage transmission through the λ5003A and the λ5100A filters, the percentage transmission through the λ5100A filter was determined. This value was then checked on the calibration curve of the λ5100A filter (Figure 2.7) and was found to be exactly the value expected at the given λ, consistent with the conclusion that the λ5100A filter did not show a measurable shift during the observational period. With the calibration curve of the λ5003A filter, Figure 2.6, and the percentage transmission as found above, the peak of the filter was located at λ5002.25A, very near the assumed straigth line variation. For the Orion observations, the filter characteristics were taken as having a peak position at λ5003.5A and the transmission at λ5006.8A as 43.1 per cent. A variation of ± 0.5A — the most that was expected over the observational period — leads to a possible error of ± 2 per cent in the transmission at λ5006.8A.

Capriotti and Daub (1960) give values for the continuum flux at H_β of η UMa and α Lyr, and for the H_β emission of NGC 6210 and NGC 6543. From the visual magnitudes given by

Johnson and Morgan (1953), and the variation with λ of the flux distribution as given by Code (1960), the magnitude difference of ν Ori compared to both η UMa and α Lyr was found. Both led to the same value of the flux of ν Ori — consistent with Capriotti and Daub's (1960) values for η UMa and α Lyr — of 8.511×10^{-11} ergs/cm^2/sec/A. Taking the equivalent width and the percentage transmission as found from the H_β calibration curve, and the flux of a planetary nebula as given by Capriotti and Daub (1960), the magnitude of a standard star (measuring continuum only) through this H_β filter may be determined. These magnitudes compared to the magnitudes as measured, yield the amount of absorption through the H_β filter. They are: α Lyr = $0^m.44$; η UMa = $0^m.17$; and ν Ori = $0^m.01$.

3. Orion Nebula

The observations of the Orion Nebula consisted of continuous intensity tracings, made at fixed declination or right ascension, while the telescope was driven with the slow motion control through either right ascension or declination. Six runs were made, each at a different declination, in the direction of decreasing right ascension. Due to a slight drift of the telescope, the declination did not remain fixed, but decreased slightly (c.f. p.24). Each run was made through at least one star of known right ascension and declination and these stars

were then used to position the runs with respect to one and another. Each run consisted of intensity tracings made through each filter along the same path through the nebula. It required approximately one hour to make each tracing. Due to the large scale of the observing program, it was generally not possible to make repeat runs. An exception to this was made for two tracings, each with a repetition of the intensity measure through the λ5003A filter made a month later than the original tracings. Other than at the extremities of the nebula where the signal was weak and near the peak intensity where variation in signal was very rapid and sensitive to slight positioning errors, the reduced magnitudes were in agreement to within $0^m.02$. Two intensity tracings in the direction of decreasing declination were made, one through the H_β filter and one through the λ3722A filter. This run was so chosen that it intersected the six runs made in right ascension and offered a check of the values obtained in these runs. The intersection points were in agreement to within $0^m.02$. Figure 3.2 shows the Orion Nebula with superposed lines indicating the runs. Table 3.3 gives the 1950.0 coordinates for point D of each run.

4. Intensity Calculations

Since the V filter does not give 100 per cent transmission throughout its passband, the correct relation between

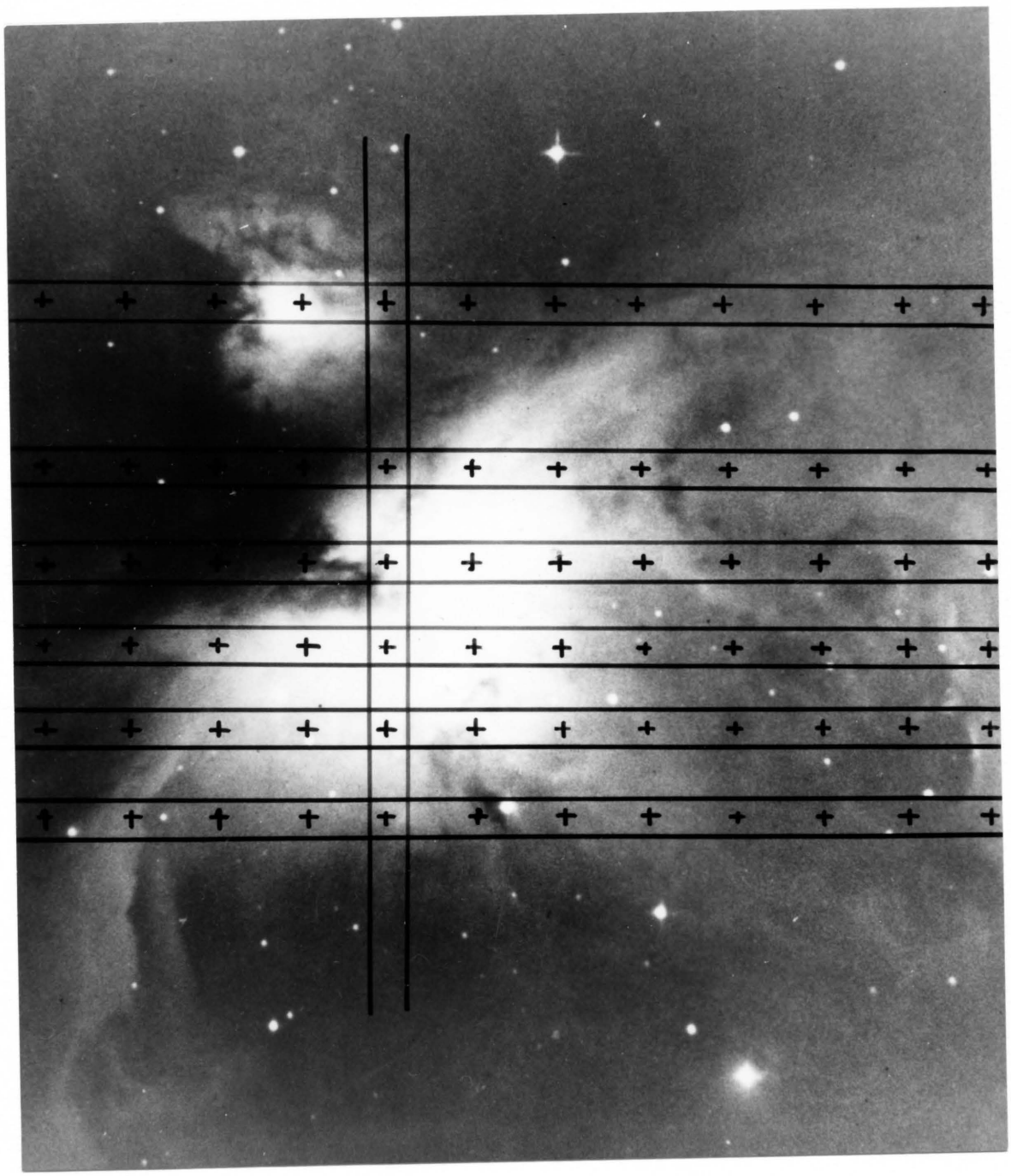

Fig. 3.2 - Position of runs made through the Orion Nebula. Marks (+) indicate points at which data reductions were made.

TABLE 3.3

1950.0 COORDINATES OF POINT D

Run	Right Ascension	Declination
1	$5^h\ 33^m\ 40^s$	$-\ 5^\circ\ 24'.4$
2	$5^h\ 33^m\ 42^s$	$-\ 5^\circ\ 26'.3$
3	$5^h\ 33^m\ 41^s$	$-\ 5^\circ\ 30'.4$
4	$5^h\ 33^m\ 40^s$	$-\ 5^\circ\ 28'.1$
5	$5^h\ 33^m\ 40^s$	$-\ 5^\circ\ 22'.0$
6	$5^h\ 33^m\ 40^s$	$-\ 5^\circ\ 17'.8$

the visual magnitudes of the sun and a star is given (Collins, Daub, and O'Dell 1961) by:

$$V^{\odot}_{\lambda 5560} - V^{*}_{\lambda 5560} = -2.5 \operatorname{Log} \frac{F^{\odot}_{\lambda 5560} \int_0^{\infty} (F^{\odot}_{\lambda}/F^{\odot}_{\lambda 5560})\, S_{\lambda}\, d\lambda}{F^{*}_{\lambda 5560} \int_0^{\infty} (F^{*}_{\lambda}/F^{*}_{\lambda 5560})\, S_{\lambda}\, d\lambda} . \qquad (3.4)$$

The quantity $\int_0^{\infty} (F^{\odot}_{\lambda}/F^{\odot}_{\lambda 5560})\, S_{\lambda}\, d\lambda$ may be evaluated by taking the distribution of the mean monochromatic intensity of the solar disc as given by Minnaert (1953) and the response curve of the visual filter as given by Johnson and Morgan (1951), and graphically integrating. The quantity $\int_0^{\infty} (F^{*}_{\lambda}/F^{*}_{\lambda 5560})\, S_{\lambda}\, d\lambda$ may be evaluated for υOri by taking the flux distribution as given by Code (1960) and the response curve given by Johnson and Morgan and graphically integrating. The ratio of the two integrals is found to be 1.024. From Minnaert's distribution of the mean monochromatic intensity, by graphical interpolation the flux received at one a.u. from the sun is found to be 1.856×10^2 ergs/cm^2/sec/A at λ5560 and 1.860×10^2 ergs/cm^2/sec/A at λ5465A. From these values for the flux, and $V^{\odot}_{\lambda 5465} = -26^{m}.73$ (Stebbins and Kron 1957), $V^{\odot}_{\lambda 5560} = -26^{m}.74$. From the visual magnitudes given by Johnson and Morgan (1953) and Code's flux distribution, $V^{*}_{\lambda 5560} = 4^{m}.64$ for υOri. The flux of υOri received at the top of the earth's atmosphere at λ5560A is found to be 5.33×10^{-11} ergs/cm^2/sec/A. Using the distribution given by Code and the flux at λ5560A as found above, the

flux per angstrom at each desired λ may be computed. The product of this flux and the equivalent width of the filter gives the flux received through a filter. It is assumed here that for ν-Ori, only continuum is measured (except for H_β which is corrected to continuum) and the variation of the continuum through the passband of the filter is negligibly small. When applied to the wide passband filters at λ5100A and λ3486A this assumption is extended to mean that any variation in the continuum to one side of the center of light of the filter — say an increase — is counter-balanced by a decrease on the other side.

The instrument magnitudes, m, as well as the magnitudes m', consistent with Code's distribution of flux through these filters are tabulated in Table 3.2. This table also contains a total instrument sensitivity based on 100 per cent for H_β.

Data reductions were made at intervals of 2 minutes of arc along each run, the intensity through each filter at each reduction point determined, and the intensities at the wavelengths of interest tabulated (Table 5.1) according to procedures and equations given under the heading of observations in Chapter V. An example of the data reduction calculations is to be found in Appendix A.

CHAPTER IV

A MODEL OF THE ORION NEBULA

1. Application of the Intensity Measures

In this chapter, a model of the Orion Nebula will be adopted and the intensity measures previously discussed will be used to derive the run of electron temperatures, electron densities, and oxygen abundance.

In models proposed by Osterbrock and Flather (1959), as well as by Menon (1961), the electron temperature was assumed to be a constant 10000°K. With this assumption, measured intensities, and a spherical model of the nebula, the electron density was determined as a function of position within the nebula. Osterbrock and Flather also considered the degree of ionization of the nebula determined from the relative strengths of the oxygen lines, with the assumption that all the oxygen was either singly or doubly ionized, and found an approximate value of $N(O)/N(H^+) = 8.3 \times 10^{-5}$.

The most commonly applied method of finding electron temperature in gaseous nebula, namely from the ratio of $I_{\lambda 4363}/I_{(N1 + N2)}$, requires no assumption to be made about the type of radiation field and can be considered independent of

electron density for densities of the order of magnitude expected in gaseous nebula. It suffers from the disadvantage of being a very difficult measure to make accurately, the ratio being of the order of 0.004 for $T_e = 10000^{\circ}K$. When interference filters are used, a measure of λ4363A is made still more difficult by its proximity to H_γ, 22A to the blue side. No attempt to measure $I_{\lambda 4363}$ was made in this investigation.

An alternate approach to determination of the electron temperature was found to be available from consideration of the expressions for the intensity of a Balmer line and for the Balmer continuous emission at the series limit. The intensity, I_λ, is given by the integral of the emission coefficient, j_λ (per unit volume), along the path length s, through the nebula such that

$$I_\lambda = \int_s \frac{j_\lambda}{4\pi}\, ds. \qquad (4.1)$$

The intensity of the Balmer line H_β is, from the emission coefficient given by Aller (1956),

$$I_{H\beta} = \frac{2.28 \times 10^{-19}}{4\pi} \int_s N_i N_e T_e^{-3/2}\, b_4 \exp(X_4)\, ds \qquad (4.2)$$

and the intensity of the Balmer continuous emission is

$$I_{Bac} = \frac{5.34 \times 10^{-22}}{4\pi} \int_s N_i N_e T_e^{-3/2} ds \qquad (4.3)$$

at the series limit. From a comparison of equations (4.2) and (4.3) it is seen that an assumption that the $b_4 \exp(X_4)$ is independent of the position along a particular path length, where both $I_{H\beta}$ and I_{Bac} are measured at the same point on the surface of the nebula, allows the ratio to be expressed as:

$$\frac{I_{H\beta}}{I_{Bac}} = \frac{2.28 \times 10^{-19}}{5.34 \times 10^{-22}} b_4 \exp(X_4) = 427\ b_4 \exp(X_4). \qquad (4.4)$$

Since, for a given type of radiation field, $b_4 \exp(X_4)$ is a function of temperature only, the ratio of the intensities is a function of electron temperature only. It should be noted that equation (4.4) is valid only if the temperature is not a function of position within the nebula. If the temperature determined at points across the nebula is found to not be constant, the resulting values are a first approximation to the real electron temperature in the usual sense of a homogeneous model being assumed to determine that a heterogeneous distribution is, in fact, the case. Figure 4.1 shows a plot of $b_4 \exp(X_4)$ as a function of temperature for both case A and case B, the curves having been constructed from values given by Seaton (1959). Figure 4.1 clearly indicates that for temperatures of $10000^{\circ}K \pm 5000^{\circ}$, an observationally determined $b_4 \exp(X_4)$ not only yields the electron temperature but also distinguishes whether the radiation may conform to case A or B.

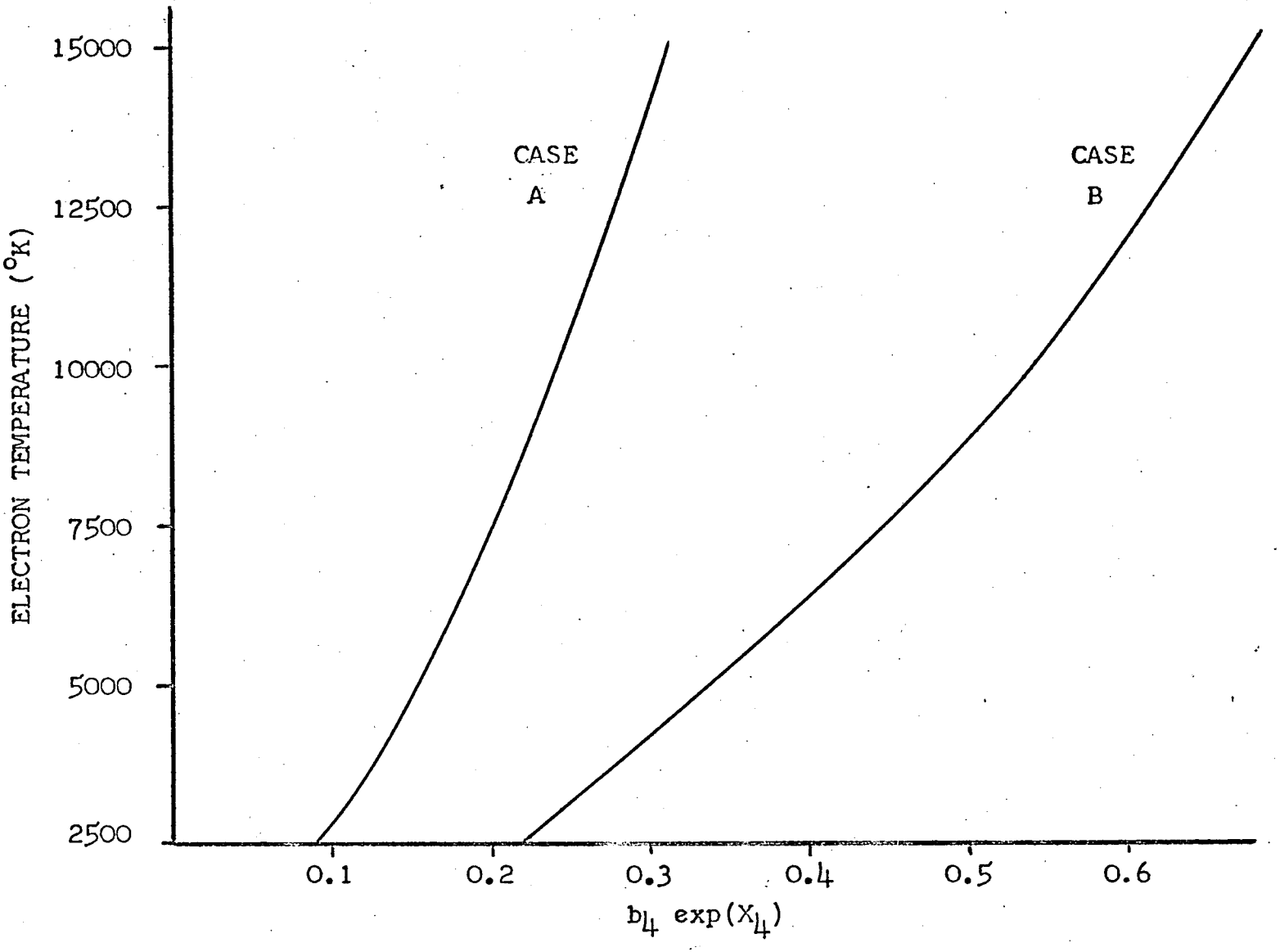

Fig.4.1 - Electron temperature vs $b_4 \exp(X_4)$ for case A and for case B.

In this investigation, since the intensities of Hβ and the visual and Balmer continuum were observed, equation (4.4) may be used if a reasonable estimate of I_{Bac} may be made. The measured intensity of the continuum to the blue side of the Balmer limit is thought to contain not only the Balmer continuum intensity, but an additional underlying continuum as well. I_{Bac} has, in the past, been determined by subtracting the visual continuum to the red side of the series limit from that to the blue side. Following the analysis made by Page (1942) in which he found the intensity of the visual continuum in planetary nebulae to be essentially independent of wavelength in the range from λ3900A to λ5000A, investigators have extrapolated the observed visual continuum to the series limit and subtracted this value from the intensity to the blue side to arrive at a value of I_{Bac} (c.f. Aller 1951). Greenstein (1946), in his discussion of the continuous emission in the Orion Nebula, similarly extrapolated the intensity in the visual continuum from λ4000A to the Balmer series limit to determine the magnitude of the Balmer discontinuity, pointing out that this extrapolation is necessary to circumvent the significant overlapping of the hydrogen lines between the series limit and λ4000A. The only known source of visual continuous emission short of λ4000A that could have a marked effect on the slope of this continuum is the two-photon

emission, which increases the intensity with decreasing wavelength. Spitzer and Greenstein (1951) have shown that 1/3 of the electron captures to the second level will go to the metastable 2s level and that the following transition to the ground state will be accomplished with two-photon emission. If the nebula is opaque to Lyman line radiation, a portion of the scattered Lyα radiation may be converted to two-photon emission if it is scattered a sufficient number of times. Consistent with results found later in this chapter that, if the choice be restricted to case A and case B, case A is to be preferred, we will assume the latter of the above mentioned processes resulting in two-photon emission to have negligible effect in the Orion Nebula. This assumption will be re-examined in section 2. of this chapter. Reference to the work of Spitzer and Greenstein shows that with this assumption, I_{Bac} may be reasonably well approximated as $I_{\lambda 3486} - I_{\lambda 4217}$ for electron temperatures of $10000^{o} \pm 5000^{o}K$. Equation (4.4) may then be used to determine, with the intensities given in Table 5.1, the electron temperature at each point for which the intensities were recorded.

From the intensity measures, the center was found to be at point L of run 4 and, assuming spherical symmetry, to have a radius of 18'. If the electron temperature and r.m.s. electron density are taken as constant along a line of sight

through the nebula, as well as $N_i = N_e$, equation (4.3) becomes

$$I_{Bac} = \frac{5.34 \times 10^{-22}}{4\pi} N_e^{\,2}\, T_e^{-3/2}\, s, \qquad (4.5)$$

where s is the distance, in centimeters, through the nebula, taken as spherical, at the point I_{Bac} is determined. The distance to the Orion Nebula is taken as 450 pc so that one minute of arc corresponds to 0.131 pc. Equation (4.5) may be rearranged as

$$N_e = \left[\frac{7.63 \times 10^{3}}{d} T_e^{\,3/2}\, I_{Bac}\right]^{\frac{1}{2}} \qquad (4.6)$$

where d is the distance through the nebula at the point considered, in parsecs. With I_{Bac}, T_e and d known, the r.m.s. electron density at each point may be found from equation (4.6).

The amount of oxygen, O^+ and O^{++}, may be calculated from the tabulated values of the intensities (Table 5.1) and the equations given by Aller (1954), the latter using the collisional cross-sections given by Seaton (1958). Since the electron density is not expected to exceed $10^3/cm^3$, the pertinent equations become:

$$\frac{N(O^+)}{N(O^{++})} = 0.298 \quad 10^{4284/T_e} \quad \frac{I_{\lambda 3727}}{I_{\lambda 5007}}\ , \qquad (4.7)$$

$$\frac{N(O^{++})}{N_e} = 4.65 \times 10^{-2} T_e^{-1} b_4 \exp(X_4) \exp(28840/T_e) \frac{I_{\lambda 5007}}{I_{H\beta}}, \qquad (4.8)$$

and agree with those given by Burbidge and Burbidge (1962) for

T_e = 10000°K. Since all the oxygen may be assumed to be either O^+ or O^{++}, the degree of ionization, y, is given by Osterbrock and Flather (1959) to be

$$y = \frac{N(O^{++})}{N(O)} = \left[\frac{N(O^+)}{N(O^{++})} + 1\right]^{-1}. \qquad (4.9)$$

Equations (4.6), (4.8) and (4.9) may then be combined to give a value for N(O) at each point of interest.

Table 4.1 lists the values, determined according to the above procedures, of $b_4\exp(X_4)$, T_e, d, N_e, $N(O^+)/N(O^{++})$, y, and N(O). Figure 4.2 shows lines of constant electron temperature, calculated on the basis of case A and interpolated from the values given in Table 4.1, superposed on a photograph of the Orion Nebula. Similarly, Figure 4.3 shows interpolated lines of constant r.m.s. electron density.

2. Discussion of the Results

From Table 4.1 and Figure 4.1 it is found that case B is not applicable to the Orion Nebula while case A yields electron temperatures of the order of magnitude of those expected in the Orion Nebula and accordingly, the determination of T_e in Table 4.1 is made assuming the nebula to be transparent to Lyman line radiation. It should be noted that theoretical objections to case A being applied to the Orion Nebula seem to be quite formidable (c.f. Osterbrock 1962),

TABLE 4.1

VALUES DERIVED WITH A CASE A MODEL OF THE ORION NEBULA

Point	$b_4 \exp(X_4)$	T_e (°K)	d(pc)	N_e (/cm^3)	$\frac{N(O^+)}{N(O^{++})}$	y	N(O) (/cm^3)
Run 1							
E	0.088						
F	0.181	6300	3.34	28	1.20	0.45	0.021
G	0.154	5000	3.77	10			
H	0.137	4200	4.10	12	0.78	0.72	0.007
I	0.165	5500	4.32	64	1.71	0.37	0.190
J	0.208	7800	4.48	154	0.66	0.60	0.049
K	0.234	9500	4.57	374	0.39	0.72	0.056
L	0.213	8000	4.60	159	0.95	0.51	0.035
M	0.180	6200	4.57	96	1.68	0.37	0.080
N	0.169	5700	4.49	72	2.21	0.31	0.110
O	0.199	7400	4.33	73	2.45	0.29	0.026
P	0.238	9700	4.10	93	2.57	0.28	0.032
Q	0.228	9000	3.79	89	5.23	0.16	0.012
R	0.215	8300	3.38	56	1.99	0.33	0.011
S	0.193	7000	2.80	48	2.17	0.32	0.021
Run 2							
E	0.213	8000	2.90	30	1.17	0.46	0.006
F	0.367						
G	0.188	6800	3.88	63	1.29	0.44	0.026

TABLE 4.1 - Continued

Point	$b_4 \exp(X_4)$	T_e (°K)	d(pc)	N_e (/cm^3)	$\frac{N(O^+)}{N(O^{++})}$	y	N(O) (/cm^3)
H	0.177	6100	4.18	93	1.54	0.39	0.078
I	0.227	9000	4.41	228	1.57	0.39	0.027
J	0.182	6400	4.57	308	1.01	0.50	0.280
K	0.203	7700	4.66	319	0.39	0.72	0.110
L	0.223	8700	4.69	178	0.47	0.68	0.028
M	0.189	6700	4.66	98	1.08	0.48	0.049
N	0.206	7700	4.57	82	1.30	0.43	0.021
O	0.234	9500	4.42	82	1.18	0.46	0.007
P	0.228	9200	4.19	83	2.65	0.27	0.010
Q	0.272	11700	3.89	114	3.05	0.25	0.047
R	0.185	6500	3.48	58	6.58	0.13	0.044
S	0.173	5800	2.93	46	2.94	0.25	0.064
T	0.153	4800	2.10	46			
Run 3							
D							
E	0.197	7300	2.89	37	1.51	0.40	0.011
F							
G	0.276	11900	3.87	39	9.34	0.10	0.002
H	0.232	9300	4.18	121	4.31	0.19	0.010
I	0.227	9000	4.40	117	3.22	0.24	0.010
J	0.180	6200	4.56	82	2.30	0.30	0.006

TABLE 4.1 - Continued

Point	$b_4 \exp(X)$	T_e (°K)	d(pc)	N_e (/cm^3)	$\frac{N(O^+)}{N(O^{++})}$	y	N(O) (/cm^3)
K	0.172	5700	4.65	63	2.53	0.28	0.088
L	0.192	6800	4.66	76	2.25	0.31	0.029
M	0.182	6400	4.65	72	3.80	0.21	0.055
N	0.188	6600	4.55	56	3.55	0.22	0.048
O	0.205	7600	4.40	60	4.48	0.19	0.016
P	0.230	9200	4.17	57	3.69	0.21	0.068
Q	0.195	7000	3.87	65	9.11	0.10	0.028
R	0.200	7400	3.45	50	5.94	0.14	0.016
S	0.190	6700	2.87	46	7.18	0.12	0.028
T	0.156	4900	2.06	46	2.91	0.25	0.087
U	0.141	4300					
Run 4							
D	0.092						
E	0.292						
F	0.186	6500	3.52	38	1.93	0.34	0.028
G	0.127	3700	3.92	50	7.89	0.11	0.360
H	0.181	6200	4.22	125	7.85	0.11	0.120
J	0.188	6600	4.60	153	2.46	0.29	0.089
K	0.193	6900	4.69	143	1.71	0.37	0.074
L	0.151	4700	4.72	84	3.03	0.25	0.640
M	0.157	5000	4.69	71	1.78	0.36	0.190

TABLE 4.1 - Continued

Point	$b_4 \exp(X_4)$	T_e (°K)	d(pc)	N_e (/cm^3)	$\frac{N(O^+)}{N(O^{++})}$	y	N(O) (/cm^3)
N	0.177	6000	4.60	64	3.50	0.22	0.083
O	0.206	7600	4.45	66	2.68	0.27	0.021
P	0.169	5700	4.22	51	6.75	0.13	0.012
Q	0.227	9000	3.92	90	6.57	0.13	0.012
R	0.124	3500	3.52	39	39.05	0.02	
S	0.253	10400	2.96	54	1.89	0.34	0.004
T	0.184	6400	2.16	43	3.15	0.24	0.024
U	0.094						
Run 5							
G	0.093						
H	0.169	5600	3.87	30	1.56	0.39	0.004
I	0.136	4200	4.11	43	2.45	0.29	0.770
J	0.171	5800	4.28	105	1.26	0.44	0.150
K	0.201	7400	4.38	177	1.34	0.43	0.058
L	0.185	6500	4.42	119	1.65	0.38	0.069
M	0.195	7100	4.39	86	1.26	0.44	0.031
N	0.228	8900	4.29	86	1.41	0.41	0.010
O	0.219	8500	4.13	88	2.41	0.29	0.014
P	0.192	7300	3.90	75	3.76	0.21	0.029
Q	0.185	6400	3.57	61	3.69	0.22	0.046
R	0.213	8100	3.12	47	2.35	0.31	0.010

TABLE 4.1 - Continued

Point	$b_4 \exp(X_4)$	T_e (°K)	d(pc)	N_e (/cm^3)	$\frac{N(O^+)}{N(O^{++})}$	y	N(O)(/cm^3)
S	0.103						
Run 6							
G	0.109	3300	2.70	27	15.10	0.06	3.4
H	0.124	3600	3.14	22			
I	0.150	4700	3.44	105	28.8	0.04	0.350
J	0.091	2500	3.63	31			
K	0.144	4500	3.75	37	22.0	0.04	0.190
L	0.167	5500	3.79	45	1.79	0.35	0.120
M	0.174	5900	3.75	59	1.83	0.34	0.071
N	0.225	8800	3.64	73	2.18	0.31	0.011
O	0.224	8800	3.45	66	2.35	0.30	0.010
P	0.217	8400	3.16	57	2.39	0.29	0.011

Fig. 4.2 -Lines of constant electron temperature ($T_e \times 10^{-2}$°K).

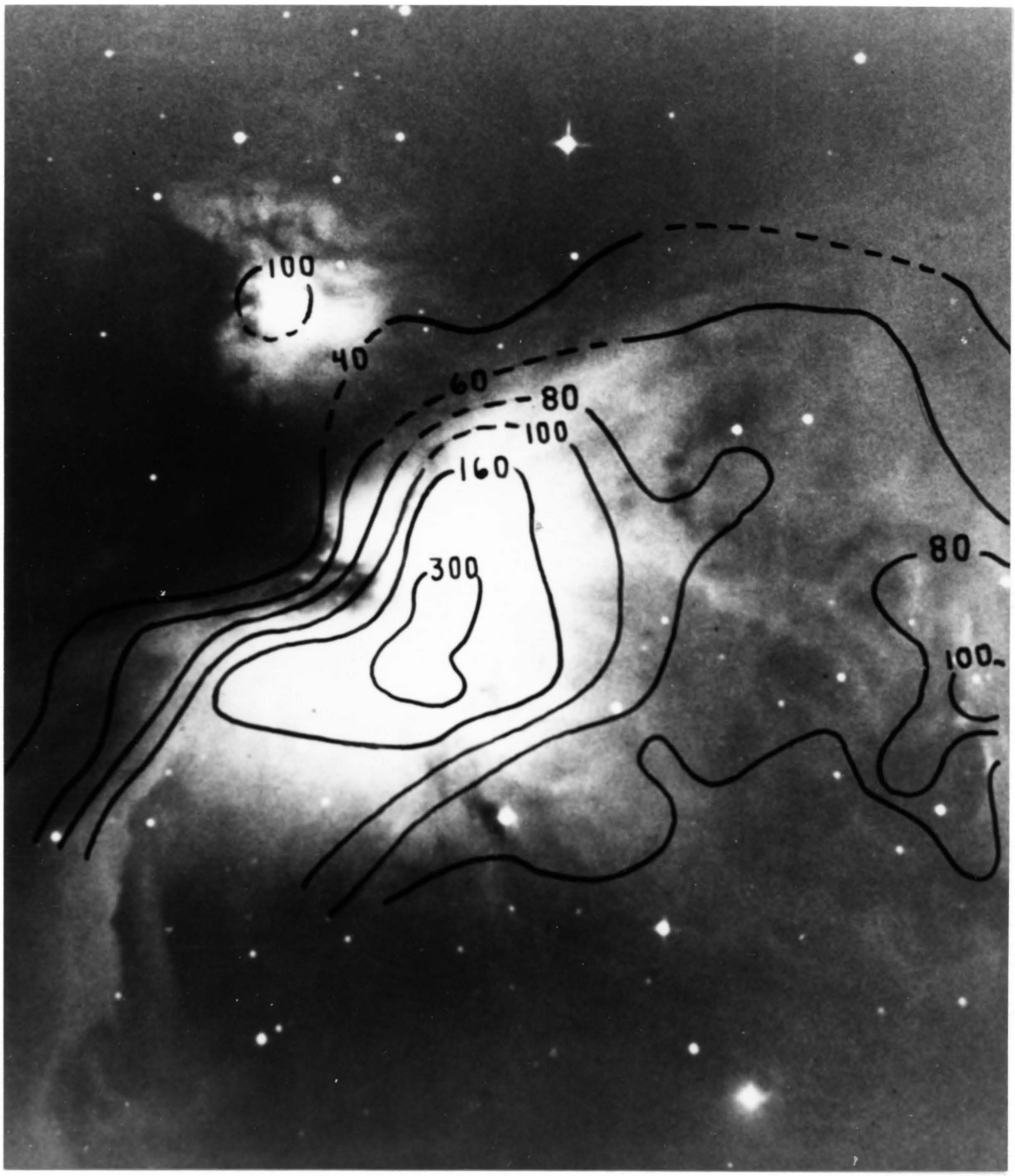

Fig. 4.3 - Lines of constant electron density.

particularly in view of the large extent of neutral hydrogen thought to surround the nebula (Menon 1958). Reference to Figure 4.1 clearly shows that any number of curves of various slopes could be fitted to the figure to satisfy the temperature condition of $10000^{\circ} \pm 5000^{\circ}K$ for the range of $b_4 \exp(X_4)$ found from these observations. Nonetheless, in existing theory, only case A satisfies the condition on the temperature, and with case B eliminated, we use case A provisionally as the only alternative, being aware that it is quite possible that this is too simple a theory to adequately describe the physical processes occurring in this nebula.

The work of Spitzer and Greenstein presents two significant considerations that merit a more careful investigation with regard to the calculations made here. They are the slope of the visual continuum near the series limit and the magnitude of the Balmer discontinuity, both as effected by the two-photon process. Spitzer and Greenstein have calculated the intensity, as a function of wavelength, of the continuum to be expected on the basis of hydrogen recombination alone, of the two-photon process (neglecting conversion of $Ly\alpha$ radiation) alone, and the sum of the two, as well as the case where all of the $Ly\alpha$ radiation is converted to two-photon emission. For the case of hydrogen recombination and two-photon emission (without $Ly\alpha$ conversion), the predicted slope of the visual

continuum agrees well with that found in Table 5.1, considering the intensities of the continuum at λ5100A and λ4217A, but the predicted magnitude of the Balmer discontinuity is much greater than that found here. On the other hand, if Lyα conversion to two-photon emission be included, the predicted and observed magnitudes of the Balmer discontinuity are in reasonable agreement, but the slope of the visual continuum does not agree with that found here. It is to be noted that with or without Lyα conversion to two-photon emission, the increased intensity of the visual continuum near the series limit is not sufficient to allow the possibility of case B, and if case A is applicable, there will be no Lyα conversion to two-photon emission. Greenstein (1946) has concluded that very probably a portion of the visual continuum is caused by scattering and reflection from dust particles in the Orion Nebula and that the true Balmer discontinuity will be greater than the observed value. The disparities considered above are then resolved if no Lyα conversion to two-photon emission be allowed and if a large portion of the visual continuum intensity be attributed to scattering and reflection of starlight, this being the common view.

It is instructive to examine the amount of light scattered and reflected that, if present in the wavelength range of the I_{Bac} calculations, could affect the determination

of the ratio of $I_{H\beta}/I_{Bac}$ an amount sufficient to show a preference for case B. To illustrate the order of magnitude of scattered light necessary to change the results in this direction, one point will be chosen, arbitrarily point L on run 1. From Table 5.1 the pertinent intensities are: I(λ3486) = 3.20-5, I(λ4217) = 1.07-5 and I(Hβ) = 1.94-3 , where the last number and the sign preceding it indicates power of ten. From these values, I_{Bac} = 2.13-5 and $b_4 exp(X_4)$ = 0.213 and with Figure 4.1 for case A, T_e = 8000°K and for case B, T_e = 2400°K. To have case B at a temperature of 8000°K, $b_4 exp(X_4)$ = 0.470 and I_{Bac} would need be 0.97-5.

With regard to the measured intensities, one expects the tendency of the continuum to become more blue due to diffuse starlight to be offset by the reddening of transmission through the interstellar medium. If we make the reddening corrections for point L of run 1 in the manner suggested by Mathis (1957), assuming that near the Trapezium only half the absorption correction derived from the stars is to be applied to the nebular intensities, the pertinent quantities become: I(λ3486) = 4.46-5, I(λ4217) = 1.34-5, and I(Hβ) = 2.19-3, from which I_{Bac} = 3.12-5 and $b_4 exp(X_4)$ = 0.164. The results of this correction alone obviously show an even greater divergence from case B. From Spitzer and Greenstein's (1951) work one would expect an increase of the 2-photon continuum of

approximately 20 per cent, at λ3486A, of the intensity of the two-photon emission at λ4217A. If the following conditions were to be assumed, namely that reddening is negligible, that none of the intensity measured at λ4217A is due to scattered light, and that the increase in the intensity of the continuum due to the two-photon process going toward λ3486A is 20 per cent of the total intensity at λ4217A, Figure 4.4 shows that the intensity of the scattered light at λ3486A would need be 50 per cent of the actual Balmer continuum intensity to fit case B. This value is considerably in excess of the 10 to 20 per cent suggested by Greenstein (1946). The negation of any of these obviously extreme assumptions would require the percentage of scattered light in the intensity measure at λ3486A to be greater than 50 per cent. It does not, therefore, appear at all likely that application of case B to the Orion Nebula can be justified.

The root-mean square electron densities, found in Table 4.1 and Figure 4.3 have an average value of 83 electrons /cm^3 and vary from a maximum near 370 to a low value near 30 electrons/cm^3. This range of values is discussed further in Chapter V.

The variation of the ratio of $N(O^+)/N(O^{++})$, as discussed in Chapter V, lends support to the conclusion from Figure 4.2 that the electron temperature is not likely to be

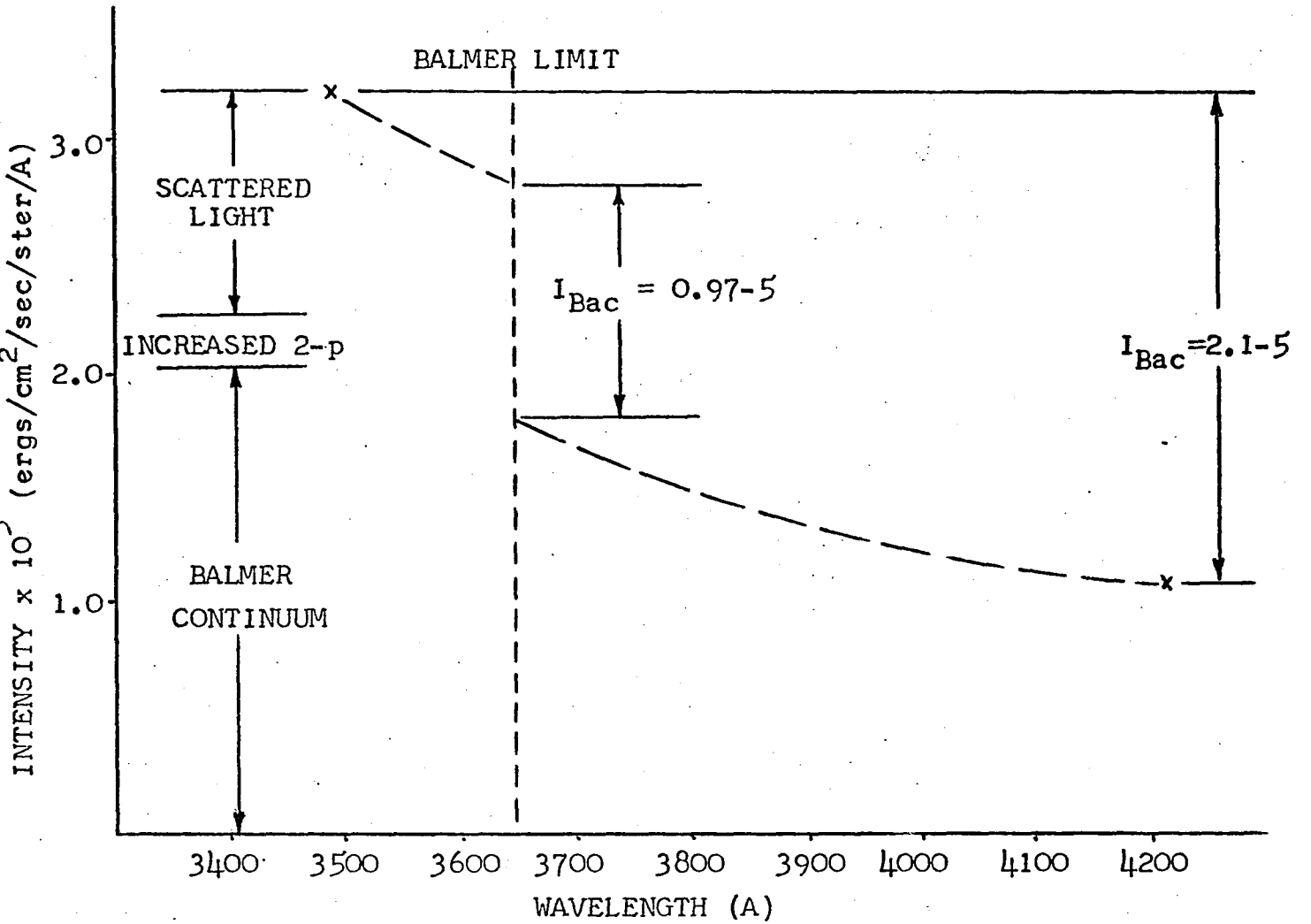

Fig.4.4 - Modification of intensities to fit case B for point L, run 1.

a constant in the Orion Nebula.

The results of this investigation may then be stated as follows. Baker and Menzel's case B is not applicable to the Orion Nebula, while electron temperatures computed on the basis of case A yield results of the order of magnitude expected. From consideration of the slope of the visual continuum it is not likely that Lyα conversion to two-photon emission makes a contribution to the intensity of the visual continuum and the observed slope of this continuum is consistent with that predicted assuming 1/3 of the electron captures to the second level reach the ground state with two-photon emission. The electron temperature in the Orion Nebula is not a constant and from a Case A model appears to be generally somewhat lower than the commonly adopted value of 10000°K.

One should be able to obtain an improved value of the average line-of-sight electron temperature from the intensities given in Table 5.1, from Figure 4.1, and from the variation of the visual continuum near the series limit as given by Spitzer and Greenstein (1951). A logical extension of this work would be to adopt a model of the nebula in which both the electron temperature and density vary as a function of position and to determine the functional relationships that satisfy both the intensities and the values of these quantities found at the outer limit of the nebula.

CHAPTER V

PHOTOELECTRIC OBSERVATIONS OF THE ORION NEBULA AT SEVEN WAVELENGTHS

This chapter presents the abstract and text of a paper on the dissertation topic that has been submitted for publication to the Astrophysical Journal.

Abstract

The intensities at selected wavelengths from λ3486A to λ6564A were measured at eighty-eight points in the Orion Nebula and are here tabulated. Electron temperature was determined at each point from the ratio of $I(H\beta)/I_{Bac}$. The results indicate a preference for Baker and Menzel's case A (transparent to Lyman line radiation) in which the temperatures vary from 3500° to 11700°K, though uncertainties in the extrapolation to determine I_{Bac} and theoretical difficulties for the Orion Nebula prevent a conclusive statement as to the applicability of case A. For an assumed model of 18' radius, the root-mean-square electron density, computed ignoring density variations along the line of sight, is found to vary from 370 to 30 electrons/cm^3. The ratio of $N(0)/N_e$ has an average value of 6.5×10^{-4}. A section in the western part and another in the southeastern

part of the nebula appear to be both deficient in O^{++} and to have higher temperatures than the neighboring areas. Both the temperature as determined here and the variation in the ratio of $N(O^{+})/N(O^{++})$ indicate that the assumption of a constant temperature throughout the nebula is invalid, and that the temperature does vary as a function of position within the nebula.

I. Introduction

Extensive surveys of the Orion Nebula have been made both spectrographically (Osterbrock and Flather 1959) and with radio observations (Menon 1961). With a photoelectric spectrophotometer, Boyce (1963) has observed the intensity of H_{β} and the Balmer decrement in the bright part of the nebula.

Osterbrock and Flather (1959) assumed a spherical model, centered at the Trapezium, with a radius of 24' and a constant electron temperature of 10000°K. The obtained a density distribution of from 1.8×10^{4} electrons/cm^3 at the center to 2.6×10^{2} electrons/cm^3 at the edge in clouds filling 1/30 of the volume.

Menon (1961) obtained a detailed intensity distribution across the nebula at 3.75 cm wavelength. For an assumed model with a constant electron temperature of 10000°K, he found a range of densities of from 2.3×10^{3} to 10 electrons/cm^3.

Boyce (1963) measured the intensity of H_β based on the absolute flux system of Code (1960), in selected areas near the Trapezium. He found that self absorption in the Balmer lines is negligible.

The need for more extensive optical observations has been expressed by many inverstigators in this field. This work was undertaken to make available such observations, both of selected emission lines and of continuum measures, at points throughout the nebula.

II. Observations

A Photoelectric photometer, with a refrigerated RCA 1P21 photocell, was used at the Cassegrain position of the 36 inch telescope of the Steward Observatory. The characteristics of the seven filters, determined from response curves made with a recording spectrophotometer are given in Table 2.1. The λ3486A glass filter was purchased through the Fish-Shurman Corporation, the λ3722A filter was an interference filter made by Spectrolab, Inc., and the remaing five interference filters were made by Baird Atomic. The filters were used by placing each of them in the light path and driving the telescope at a constant rate (0.771' per minute of time) across the nebula, while continuously recording the intensity on a strip chart recorder. Runs across the nebula in the direction of decreasing

right ascension were made with each filter at six different declinations. One run, with the λ4857A and λ3722A filters, was made at constant right ascension in the direction of decreasing declination and intersecting each of the other runs. The hour angle was restricted to within ± 2 hours to minimize the effect of atmospheric absorption. Two stars, taken as standard stars, were observed through each filter at the beginning and end of each night's observations, and used to correct for atmospheric extinction in the data reductions. The flux distribution of one of these stars, υOri, is given by Code (1960), and using the method given by Collins, Daub, and O'Dell (1961), the nebular intensities were put on the "absolute" flux system of Code. The magnitude of υOri is taken as V = $4^m.59$ (Johnson and Morgan 1953) and at λ5560A, the flux/A of υOri = 5.33×10^{-11} ergs/cm^2/sec/A. Table 3.2 lists, for each filter, the flux/A at the appropriate wavelength and the product of the equivalent width and the flux/A to give the flux received through the filter. The measured magnitudes of υOri were taken as pure continuum measures, with the exception of the λ4857A filter, which was corrected by comparison of the planetary measures of Capriotti and Daub (1960) with those made by the writer. Only a small amount of depression of the continuum ($0^m.01$) due to H_β absorption was found through this filter. Using the product of the equivalent width and the flux/A, the instrument magnitude of υOri

corrected for extinction, and the instrument magnitude of the nebula corrected for extinction, the flux from the nebula through each filter was determined. The flux was converted to the intensity by dividing it by the area appropriate to a diaphragm size of 1'. Observations were also made of planetary nebulae NGC 6210 and NGC 6543 to afford a check on the consistency of the data reductions, as well as standard stars αLyr and ηUMa whose flux distribution is given by Code (1960). Agreement with log F(N1) and log F(Hβ) as determined by Collins et al. (1961) was found to be within their suggested probable error.

Due to the size of the observing program, only a few repeat runs could be made. Other than at the extremities of the nebula where the signal was weak and at one point near the center where the signal changes rapidly, agreement to within $0^m.02$ on runs made a month apart was found. The intersection points of the runs made at constant right ascension with those made at constant declination were in agreement to within $0^m.02$.

Data reductions were made for points spaced 2' apart along each run. For run 1, the 1950.0 right ascensions of points D, E, ..., U at which data reductions were made are $5^h33^m40^s$, $5^h33^m32^s$, ..., $5^h31^m24^s$. The declination did not remain precisely constant but decreased uniformily at the rate of 0.0225' per 2' interval along each run. Table 3.3 gives the

1950.0 coordinates for point D of each run, from which — with the above information — the coordinates of each point on each run may be determined.

In determining the intensities of the desired emission and continuum measures, unwanted emission within the passband of each filter was removed using the relative intensities given by Aller and Liller (1959) and Wyse (1942). The transmission of H_α through the λ6564A filter is 38 per cent. Since the sensitivity of this measure is poor, as is the equivalent width small, no correction is made for continuum background, and the resulting relation is

$$I(\lambda 6564A) = 0.38\ I_{H_\alpha}. \qquad (5.1)$$

For the λ5100A filter, the transmission of the N1 line at λ5007A is 45.6 per cent and of the N2 line at λ4959A is 6.6 per cent (taking N1/N2 = 3, this is 2.2 per cent of N1). With 160.1A of continuum at λ5100A,

$$I(\lambda 5100A) = S(0.478)\ I_{N1} + 160.1\ I_{\lambda 5100}\ , \qquad (5.2)$$

where S is a sensitivity correction for the sensitivity at λ5007A rather than at λ5100A and is 0.876/0.81. The transmission of the N1 line through the λ5003A filter is 43.1 per cent and of the N2 line is 1.2 per cent, with the resulting relation that

$$I(\lambda 5003A) = 0.435\ I_{N1} + 12.4\ I_{\lambda 5100}\ , \qquad (5.3)$$

where the continuum at λ5003A is taken equal to that at λ5100A.

The transmission of I_{H_β} through the λ4857A filter is 40.5 per cent and the continuum at H_β is found from a straight line interpolation of the values at λ5100A and λ4217A, with the result that

$$I(\lambda 4857A) = 0.405\ I_{H\beta} + 10.2\left[I_{\lambda 4217} - 0.729(I_{\lambda 4217} - I_{\lambda 5100})\right] . \qquad (5.4)$$

The λ4217A filter measures continuum only, so that

$$I(\lambda 4217A) = 19.8\ I_{\lambda 4217} . \qquad (5.5)$$

The transmission through the λ3722A filter is 38.9 per cent of the line at λ3726A and 38.3 per cent of the line at λ3729A, from which an average value of 38.6 per cent is taken for the O^+ doublet. The relative strength of the other lines (with respect to the sum of both components of λ3727A) multiplied by the percentage transmission of each line within the passband and summed over all these lines is 10.7 per cent, and taking the continuum strength at λ3727A as equal to that at λ4217A, the resulting relation is

$$I(\lambda 3727A) = 0.493\ I_{O+} + 18.1\ I_{\lambda 4217} . \qquad (5.6)$$

The transmission of the λ3486A filter is 2 per cent at λ3354A and at λ3650A. Reference to a microphotometer tracing of the spectrum of the Orion Nebula in this range (Greenstein 1946) shows no strong lines present. The O^+ doublet at λ3727A does, however, have 0.7 per cent transmission through the wing of this filter. Accordingly, this filter is taken as measuring

continuum plus a small contribution from O^+, such that

$$I(\lambda 3486A) = 43.7\ I_{\lambda 3486} + 0.007\ I_{O^+} . \qquad (5.7)$$

The resulting intensities of O^{++} at λ5007A, O^+ at λ3727A, H_α and H_β in ergs/cm^2/sec/ster and the continuum intensities at λ5100A, λ4217A, and λ3486A in ergs/cm^2/sec/ster/A are given in Table 5.1 where the last digit in each column, and the minus sign preceding it, indicates power of ten.

III. Temperatures

In nebula, electron temperature is commonly determined from the ratio of the intensities of the lines of O^{++}, namely $I(\lambda 4363A)/I(N1 + N2)$(Menzel, Aller and Hebb 1941). For a temperature of 10000°K this ratio is difficult to measure accurately, being of the order of 0.004. When using narrow band interference filters, a measure of $I(\lambda 4363)$ is further complicated by H_γ being only 22A to the blue side of this line. Because of these difficulties, and because an independent temperature determination is desirable, electron temperature is here found from the ratio of the intensity of H_β to the intensity of the Balmer continuum at the series limit. This ratio is given by (c.f. Aller 1956)

$$\frac{I(H_\beta)}{I_{Bac}} = \frac{2.28 \times 10^{-19} N_i N_e T_e^{-3/2} b_4 \exp(X_4)}{5.34 \times 10^{-22} N_i N_e T_e^{-3/2}}$$

$$= 427\ b_4 \exp(X_4) . \qquad (5.8)$$

TABLE 5.1

INTENSITY MEASURES

Point	$I_{\lambda 5007}$	$I_{\lambda 3727}$	$I_{\lambda 5100}$	$I_{\lambda 4217}$	$I_{\lambda 3486}$	$I_{H\beta}$	$I_{H\alpha}$
Run 1							
E	7.28-5	4.44-5	5.91-7	5.50-7	6.28-7	2.91-5	
F	1.41-4	1.22-4	9.44-7	6.30-7	1.33-6	5.41-5	
G	1.90-4	1.71-4	1.32-6	9.45-7	1.08-6	8.55-5	
H	4.21-4	5.19-4	3.23-6	3.40-6	6.10-6	1.59-4	9.31-4
I	1.27-3	1.18-3	7.15-6	7.44-6	1.31-5	3.99-4	2.29-3
J	6.84-3	3.69-3	2.28-5	1.68-5	3.71-5	1.81-3	8.98-3
K	3.97-2	1.90-2	1.23-4	3.50-5	1.26-4	9.05-3	3.17-2
L	4.83-3	4.52-3	1.66-5	1.07-5	3.20-5	1.94-3	5.14-3
M	1.88-3	2.19-3	6.83-6	4.95-6	1.62-5	8.67-4	2.61-3
N	1.13-3	1.51-3	5.11-6	4.55-6	1.17-5	5.19-4	1.55-3
O	6.74-4	1.48-3	2.94-6	2.73-6	7.57-6	4.12-4	1.14-3
P	5.25-4	1.67-3	2.27-6	2.07-6	6.91-6	4.92-4	1.55-3
Q	3.15-4	1.87-3	1.70-6	1.53-6	6.10-6	4.45-4	1.38-3
R	2.66-4	5.51-4	1.64-6	1.40-6	3.23-6	1.67-4	
S	2.09-4	3.76-4	1.33-6	8.91-7	2.34-6	1.19-4	
Run 2							
E	9.33-5	1.08-4	7.95-7	9.15-7	1.38-6	4.61-5	
F	1.94-4	1.73-4	1.22-6	1.83-6	2.36-6	8.21-5	
G	5.77-4	5.95-4	3.79-6	4.16-6	7.71-6	2.85-4	9.43-4

TABLE 5.1 - Continued

Point	$I_{\lambda 5007}$	$I_{\lambda 3727}$	$I_{\lambda 5100}$	$I_{\lambda 4217}$	$I_{\lambda 3486}$	$I_{H\beta}$	$I_{H\alpha}$
H	1.58-3	1.65-3	9.86-6	1.33-5	2.32-5	7.46-4	2.20-3
I	4.43-3	7.94-3	1.64-5	2.61-5	6.15-5	3.42-3	8.88-3
J	3.21-2	2.38-2	2.28-4	4.64-5	1.57-4	8.60-3	3.90-2
K	3.66-2	1.32-2	2.55-4	3.60-5	1.28-4	7.94-3	3.54-2
L	7.69-3	3.94-3	1.95-5	1.09-5	3.50-5	2.29-3	6.84-3
M	2.11-3	1.78-3	5.48-6	5.61-6	1.62-5	8.58-4	2.28-3
N	1.03-3	1.27-3	3.98-6	4.27-6	1.01-5	5.10-4	1.33-3
O	6.85-4	1.05-3	2.20-6	2.49-6	6.74-7	4.25-4	9.44-4
P	4.91-4	1.51-3	2.15-6	1.78-6	6.04-6	4.16-4	1.02-3
Q	4.35-4	1.95-3	2.93-6	1.86-6	6.40-6	5.39-4	1.41-3
R	2.06-4	1.01-3	1.23-6	1.15-6	4.10-6	2.33-4	
S	2.49-4	4.56-4	1.38-6	1.29-6	3.17-6	1.39-4	
T	1.51-4	2.23-4	9.87-7	9.34-7	2.03-6	7.15-5	
Run 3							
D	7.46-5	1.11-4	5.21-7		1.06-6	4.46-5	
E	1.32-4	1.80-4	9.03-7	9.90-7	1.82-6	6.97-5	
F	4.17-4	4.76-4	5.99-6	7.63-6	7.64-6	1.59-4	
G	2.32-4	3.22-3	3.88-6	3.59-6	9.70-6	7.18-4	1.71-3
H	5.26-4	2.67-3	3.74-6	4.60-6	1.35-5	8.84-4	2.00-3
I	6.75-4	2.47-3	4.89-6	5.60-6	1.49-5	9.29-4	2.00-3
J	9.10-4	1.45-3	5.99-6	6.16-6	1.43-5	6.29-4	1.30-3

TABLE 5.1 - Continued

Point	$I_{\lambda 5007}$	$I_{\lambda 3727}$	$I_{\lambda 5100}$	$I_{\lambda 4217}$	$I_{\lambda 3486}$	$I_{H\beta}$	$I_{H\alpha}$
K	7.47-4	1.14-3	4.15-6	4.63-6	1.02-5	4.10-4	1.06-3
L	7.96-4	1.44-3	4.20-6	3.75-6	1.00-5	5.13-4	1.22-3
M	5.98-4	1.66-3	3.03-6	2.79-6	8.90-6	4.75-4	1.10-3
N	3.93-4	1.07-3	2.06-6	2.17-6	5.70-6	2.83-4	
O	2.52-4	1.05-3	1.64-6	1.33-6	4.47-6	2.75-4	
P	1.84-4	7.91-4	9.00-7	8.56-7	2.90-6	2.00-4	
Q	1.61-4	1.22-3	9.74-7		3.63-6	3.02-4	
R	1.07-4	5.69-4	6.70-7		1.76-6	1.50-4	
S	8.72-5	4.88-4	5.15-7		1.45-6	1.18-4	
T	9.91-5	3.95-4	8.32-7		1.67-6	1.12-4	
U	6.27-5	2.35-4	4.30-7		9.01-7	5.42-5	
Run 4							
D	7.88-5	1.36-4	4.60-7		1.18-6	4.64-5	
E	1.21-4	1.52-4	8.69-7	1.31-6	1.78-6	5.89-5	
F	2.19-4	3.16-4	1.55-6	2.01-6	3.26-6	9.96-5	
G	6.02-4	1.12-3	4.30-6	4.99-6	1.07-5	3.08-4	1.13-3
H	9.75-4	5.30-3	7.89-6	9.85-6	2.77-5	1.38-3	3.73-3
J	3.44-3	6.46-3	1.80-5	1.77-5	4.42-5	2.13-2	6.59-3
K	4.10-3	5.73-3	1.71-5	1.37-5	3.56-5	1.81-3	6.16-3
L	2.37-3	2.99-3	9.10-6	7.09-6	2.06-5	8.73-4	2.60-3
M	1.22-3	1.94-3	4.92-6	4.53-6	1.32-5	5.79-4	1.39-3

TABLE 5.1 - Continued

Point	$I_{\lambda 5007}$	$I_{\lambda 3727}$	$I_{\lambda 5100}$	$I_{\lambda 4217}$	$I_{\lambda 3486}$	$I_{H\beta}$	$I_{H\alpha}$
N	6.79-4	1.56-3	2.93-6	2.23-6	7.52-6	4.01-4	1.04-3
O	5.19-4	1.29-3	2.74-6	2.41-6	6.27-6	3.39-4	
P	2.74-4	1.12-3	1.38-6	1.17-6	4.46-6	2.38-4	
Q	2.67-4	2.00-3	1.64-6	1.53-6	6.35-6	4.67-4	1.31-3
R	1.26-4	1.00-3	9.58-7	1.17-6	4.59-6	1.82-4	
S	1.69-4	4.20-4	1.20-6	1.54-6	2.60-6	1.14-4	
T	1.17-4	2.69-4	1.06-6	9.99-7	2.00-6	7.90-5	
U	7.24-5	1.78-4	6.84-7		1.23-6	4.96-5	
Run 5							
G	4.45-5		6.44-7		9.63-7	3.80-5	
H	1.73-4	1.57-4	1.08-6	1.19-6	2.30-6	8.01-5	
I	7.64-4	6.07-4	4.37-6	4.24-6	7.88-6	2.12-4	8.75-4
J	2.91-3	2.30-3	1.47-5	1.46-5	2.74-5	9.38-4	7.48-3
K	5.60-3	6.76-3	1.80-5	1.54-5	4.38-5	2.44-3	7.88-3
L	2.42-3	2.97-3	1.05-5	1.01-5	2.58-5	1.24-3	4.06-3
M	1.23-3	1.31-3	5.45-6	5.39-6	1.26-5	5.99-4	1.99-3
N	9.51-4	1.52-3	3.63-6	3.07-6	9.19-6	5.95-4	1.59-3
O	6.39-4	1.65-3	2.33-6	2.03-6	7.41-6	5.04-4	1.35-3
P	4.72-4	1.57-3	2.18-6	2.18-6	6.79-6	3.79-4	1.28-3
Q	3.59-4	9.62-4	1.96-6	2.04-6	5.44-6	2.68-4	8.77-4
R	1.84-4	4.36-4	1.13-6	1.21-6	2.47-6	1.15-4	

TABLE 5.1 - Continued

Point	$I_{\lambda 5007}$	$I_{\lambda 3727}$	$I_{\lambda 5100}$	$I_{\lambda 4217}$	$I_{\lambda 3486}$	$I_{H\beta}$	$I_{H\alpha}$
S	1.37-4	2.82-4	9.98-7		1.65-6	7.29-5	
Run 6							
G	5.47-5	1.41-4	1.77-7		1.34-6	6.83-5	
H	4.15-6	1.55-4	2.69-6	2.55-6	3.48-6	4.92-5	
I	1.75-4	2.11-3	8.75-6	1.47-5	2.88-5	9.04-4	
J	1.65-4	4.36-4	3.22-6	4.37-6	8.00-6	1.41-4	
K	3.06-4	3.75-4	2.71-6	2.82-6	5.07-6	1.38-4	
L	4.71-4	4.79-4	2.83-6	2.99-6	5.49-6	1.78-4	
M	6.45-4	7.57-4	3.85-6	3.32-6	7.13-6	2.83-4	
N	4.27-4	1.03-3	2.39-6	2.61-6	5.72-6	2.98-4	
O	3.31-4	8.62-4	1.79-6	1.91-6	4.31-6	2.32-4	
P	2.56-4	6.17-4	1.59-6	1.83-6	3.61-6	1.64-4	

Two difficulties encountered in using this expression are the precise determination of the value of I_{Bac} and the choice of a proper b_4 to measure the departure from thermodynamic equilibrium. The intensity to the blue side of the Balmer limit is thought to contain not only Balmer continuous emission, but another underlying continuum consisting of contributions from the continuum of higher series, two-photon emission, etc. The intensity of the Balmer continuum is then estimated by subtracting the intensity to the red side of the Balmer limit from that to the blue side. Here, I_{Bac} is estimated as I(λ3486A) - I(λ4217A). From Table 5.1, it is seen that the visual continuum in the central portion of the nebula generally diminishes with decreasing wavelength and that if this is the case throughout the visual continuum, I_{Bac} would be underestimated. If the slopes, $dI/d\lambda$, of the visual continuum to the blue side of λ4217A and the Balmer continuum to the red side of λ3486A have opposite signs and large values, I_{Bac} as determined here will be overestimated.

When the values of b_4 for case A (no reabsorption of Lyman line radiation) and for case B (reabsorption of Lyman line radiation) were computed by Baker and Menzel (1938), they remaked that the then available observational data of planetary nebulae implied case B to be the more likely of the two. Since that time, the b_4 from case B and the electron temperature from

the relative strength of the O^{++} lines have been used in a number of nebulae to determine the electron density in the expression for $I_{H\beta}$. Seaton (1959) has recalculated the b_4's and gives values of $b_4 \exp(X_4)$ as a function of temperature for both case A and B. Given the intensities of H_β and the Balmer continuum, derived from the values in Table 5.1 according to the above procedures, the electron temperature may then be found from equation (5.8) and a plot of $b_4 \exp(X_4)$ versus temperature for both case A and B. Case A yields a temperature ranging from 3500° to 11700°K, while case B does not yield a temperature above 35000K. Of the two cases, only case A offers likely values of the temperature, though generally less than the commonly adopted value of 10000°K. A $1/\lambda$ law of interstellar absorption (for which the values used here and presented in Table 5.1 were not corrected) would reduce these temperatures to still lower values. For the two planetaries observed by the writer, this method of determining temperature indicates a temperature of approximately 6000°K with case B being applicable. To have the measures of the Orion Nebula fit case B, either $I_{H\beta}$ must be increased by a factor of 2.3 or I_{Bac} must be decreased by this same factor. In lieu of the previously mentioned agreement with the planetary measures of Collins et al. (1961), $I_{H\beta}$ is not likely to be in error by a factor of this magnitude. The uncertainty of the determination of I_{Bac} lies

primarily in the extrapolation of the visual continuum from λ4217A to the series limit at λ3646A. If I_{Bac} were to be decreased, the Balmer discontinuity would be much less than the measured value of $1^m.6$ (Greenstein 1946), while the extrapolation used here, when corrected for interstellar absorption and scattered light is in good agreement with this value. Assuming this method to offer a reasonable estimate of I_{Bac}, Figure 4.2 shows lines of constant temperature, calculated on the basis of case A and interpolated from those found at the tabulated points in the nebula, superposed on a photograph of the Orion Nebula. The photograph was taken with the Steward Observatory 36 inch telescope using a 103aO plate. It is to be noted that the electron temperature found here is an average value in the sense that, as a first approximation, the temperature is taken to be constant along the line of sight at each point to determine, from Figure 4.2, that the temperature varies as a function of position within the nebula. This variation will again be discussed in Section VI.

IV. Electron Density

With the temperature determined, the r.m.s. average electron density in the line of sight may be found from either of the equations making up the ratio of equation (5.8), a distance through the nebula at the point considered, and a

measured intensity. Taking the equation for I_{Bac} and assuming all of the hydrogen to be ionized, as well as the electrons to be contributed only by the hydrogen, one has:

$$N_e = \left[\frac{7.63 \times 10^3}{d} T_e^{3/2} I_{Bac}\right]^{\frac{1}{2}}, \qquad (5.9)$$

where d is the distance through the nebula, in parsecs, at each point considered, having assumed the nebula to be a spherical volume.

From the intensity measures, the maximum diameter of the nebula is found to be 36' and taken as spherical, the center was found to be at point L on run 4. This is slightly west and south of the center of the 3.75 cm brightness contours found by Menon (1961). With the distance to the nebula taken as 450 pc, such that 1'= 0.131 pc, the r.m.s. average electron density in the line of sight is found to vary from 370 to 30 electrons/cm^3. A $1/\lambda$ law of interstellar absorption will change the density only slightly, since the increase in I_{Bac} tends to be offset by the decrease in temperature. The maximum value near 400 electrons/cm^3 agrees with that suggested by Haddock, Mayer and Sloanaker (1954) and by Baldwin (1953). It should be noted with emphasis that the maximum given here is a maximum of the r.m.s. average line-of-sight density, where the spherical model has been used only to determine the distance through the nebula at each point and not that the density

varies in relation to distance from the center. Accordingly, this value is not directly comparable to that given by Osterbrock and Flather (1959) of by Menon (1961), and it is to be expected that individual condensations will lead to higher local values of the density than the r.m.s. maximum value found here. Interpolated lines of constant r.m.s. electron density are superposed on a photograph of the Orion Nebula in Figure 4.3.

V. Oxygen Abundance

The amount of oxygen, O^{+} and O^{++}, may be calculated from the tabulated values of the intensity and the equations given by Aller (1954), the latter reducing to the equations given by Burbidge and Burbidge (1962) when N_e does not exceed $10^3/cm^3$. The collisional cross sections are given by Seaton (1958). In this manner, $N(O^{+})/N(O^{++})$ was calculated for each of the points in Table 5.1 and was found to vary from 0.37 to 8, where the lower values were found in the vicinity of the Trapezium and the higher values in sections of the western and southeastern parts of the nebula. As was pointed out by Burbidge, Gould, and Pottasch (1963), this ratio should be relatively small when close to the exciting stars (as is the case here in the vicinity of the Trapezium) and that areas showing a relatively low amount of O^{++} should be expected to

have high electron temperatures in comparison to the surrounding areas (as reference to Figure 4.2 shows to be the case with this model in the western and southeastern parts of the nebula). It might be objected that since the ratio of $N(O^{+})/N(O^{++})$ is a function of the temperature, this result reflects only the temperature found in Figure 4.2. Such is not the case, however, as can be seen by comparing points K and Q on run 1 which have nearly the same electron temperature, but have values for this ratio, respectively, of 0.39 and 5.3. These oxygen measures indicate that regardless of whether or not case A or B is applicable, the temperature is not constant throughout the nebula. Colored photographs of the Orion Nebula show two areas that are predominantly red (c.f. Bertola 1962) and that are the same areas found here to be relatively deficient in O^{++} and to have higher electron temperatures than the surrounding areas.

By comparing the intensity of H_{β} to that of the N1 line, and using T_e, N_e, and $N(O^{+})/N(O^{++})$ found for each point in the nebula, the ratio of $N(O)/N_e$ and $N(O)$ may be calculated assuming that all the oxygen is either O^{+} or O^{++}. $N(O)/N_e$ varies from 10^{-2} to 10^{-4} with an average value of 6.5×10^{-4} and $N(O)$ ranges from 10^{-1} to $8 \times 10^{-3}/cm^3$, with an average value of $6.0 \times 10^{-2}/cm^3$.

VI. Concluding Remarks

Both the ratio of $N(O^{+})/N(O^{++})$ and that of $I_{H\beta}/I_{Bac}$ vary in such a manner as to indicate that the electron temperature is a function of position and not a constant throughout the nebula. Although the λ4363A line is difficult to measure so that it may be compared point by point with the measures made here, it is feasible to do so in at least the bright portion of the nebula and if accomplished, should show the temperature to vary. Two particular areas show a deficiency of O^{++} relative to the surrounding areas. In the intensity measures, these areas are characterized by diminishing I_{N1} while $I_{\lambda 3727}$ fluctuates and at times is substantially increased. Observations made by Faulkner (1962) indicate that this phenomenon is also likely present in the η Carina Nebula. If excitation mechanisms be restricted to case A and case B, these observations show a preference for case A and accordingly, for Lyman line radiation not being reabsorbed within the nebula. A large increase in the intensity of the visual continuum to the blue side of λ4217A would lead to higher temperatures for case A, or possibly even case B, but would result in considerable variance from the commonly used value of the Balmer discontinuity. If one were to assume that reddening to the Orion Nebula is negligible; attribute an increase in the intensity

of λ3486A of 20 per cent of the intensity of λ4217A due to the two-photon process; and assume that a portion of the intensity at λ3486A is scattered light while none of that at λ4217 is scattered light; it is found from these observations near the Trapezium that scattered light must contribute 50 per cent of the intensity of the Balmer continuum to the total measured intensity at λ3486A to have the measures fit case B. Greenstein (1946) has suggested that this intensity be between 10 and 20 per cent. The removal of any of the obviously extreme assumptions mentioned above requires an even greater amount of scattered light and accordingly, it does not appear possible to fit case B with these observations. On the other hand, it should be pointed out that the theoretical objections to case A (c.f. Osterbrock 1962) appear quite formidable, particularily in lieu of the large amount of neutral hydrogen thought to surround the nebula (Menon 1957). It is therefore concluded here that case B is not applicable to the Orion Nebula and that while case A does lead to a likely range of temperatures, its use here should be viewed with some reserve until there is better agreement with theory.

Due to low sensitivity of the photocell at wavelengths greater than λ6000A, the $I_{H\alpha}$ as measured here is not considered reliable enough for precise determination of the Balmer decrement. Neither the points nor the areas observed by Boyce (1963)

are exactly the same as those observed in this work, but by interpolation, the values of the ratio of $I_{H\alpha}/I_{H\beta}$ are in agreement with those of Boyce (1963) to within 10 per cent.

The writer would like to express his gratitude to Dr. H.M. Johnson, who directed the earlier part of this work while at Steward Observatory and maintained continued interest in it; to Dr. W. S. Fitch of the Steward Observatory for much helpful advice and assistance; to Drs. B. Lynds of Steward Observatory, A. D. Code and J.S. Mathis of Washburn Observatory and D. Osterbrock of Yerkes Observatory for beneficial discussions.

APPENDIX A

A SAMPLE INTENSITY CALCULATION

As an illustration of the method used in making the intensity calculations, the intensity of the N1 line at λ5007A will be determined in a step-by-step manner for point L of run 1. To determine the strength of the N1 line, the instrument magnitudes through the λ5003A and the λ5100A filters must be known.

The intensity measure through the λ5003A filter was made January 19, 1962 at 9:15 MST and at a local mean sidereal time of 4^h47^m. The coordinates of point L were right ascension of $5^h32^m36^s$ and declination of $-5^\circ24'.8$. The hour angle was then 0^h46^m and the sec Z = 1.290. The time since the observation on the standard star υOri was t = 39 min. The instrument deflection, at a gain of 4-4 (4 on the coarse gain and 4 on the fine gain), was 76.1 per cent and the sky deflection was 9.1 per cent corresponding, then, to a true deflection of 67 per cent. The instrument magnitude associated with a 4-4 gain was $9^m.162$ and with a 67 per cent deflection was $2^m.065$, where 10-100 per cent range corresponds to $2^m.5$. The resulting instrument magnitude was then $7^m.097$. From Table 3.1, K = $0^m.195$, $\alpha = 0^m.011$ per hour and Z.P. = $0^m.126$. Then from equation 3.1, the

instrument magnitude m_λ, corrected for extinction, is

$m_\lambda = 7^m.097 - 0^m.195(1.29) + 0^m.011(39/60) - 0^m.126$

$= 6^m.726$ (λ5003A).

In a similar manner, the instrument magnitude, corrected for extinction, of the signal through the λ5100A filter for this same point was determined to be $m_\lambda = 5^m.941$ (λ5100A).

From Section 4 of Chapter III, the magnitude of υOri through the V filter at λ5560A is $4^m.64$ and the flux received at the top of the earth's atmosphere is 5.33×10^{-11} ergs/cm^2/sec/A. From Code's (1960) energy distribution of υOri, $m(1/\lambda) = m(1/5003) = -0^m.13$, and since

$$m(\lambda) = m(1/\lambda) - 5 \log (5560/\lambda),$$

$$m(\lambda) = -0.13 - 0.228$$

$$= -0^m.358,$$

and the magnitude of υOri through the V filter at λ5003A is $m = 4^m.28$. The flux/A is given by

$$m(\lambda 5560A) - m(\lambda 5003A) = -2.5 \log (F_{\lambda 5560}/F_{\lambda 5003}), \text{ or}$$

$$4.64 - 4.28 = 2.5 \log (F_{\lambda 5003}/5.33 \times 10^{-11})$$

from which, as given in Table 3.2,

$$F_{\lambda 5003} = 7.42 \times 10^{-11} \text{ ergs/cm}^2\text{/sec/A}.$$

Similarly, the flux/A at λ5100A is 6.90×10^{-11} ergs/cm^2/sec/A.

The flux of the nebula at λ5003A may now be found by comparing the instrument magnitudes of the nebula and of υOri, and knowing the flux of the star (Table 3.2), one finds the

flux from the nebula as

$$m^n - m^* = 2.5 \log F^*/F^n \quad \text{or}$$

$$6.726 - 4.781 = 2.5 \log (9.2 \times 10^{-10}/F^n),$$

from which

$$F^n(\lambda 5003A) = 1.53 \times 10^{-10} \text{ ergs/cm}^2\text{/sec.}$$

Since the intensity is the flux per unit solid angle and the diaphragm is θ = 1'diameter, the corresponding solid angle is $\pi\theta^2/4$ and the intensity $I = 1.5 \times 10^7 F$, from which

$$I(\lambda 5003A) = 2.30 \times 10^{-3} \text{ergs/cm}^2\text{/sec/ster.}$$

Similarly,

$$I(\lambda 5100A) = 5.16 \times 10^{-3} \text{ergs/cm}^2\text{/sec/ster.}$$

To determine the intensity of the N1 line for this point L of run 1, Equations (5.2) and (5.3) are solve simultaneously, i.e.

$$I(\lambda 5100A) = 0.518\ I_{N1} + 160.1\ I_{\lambda 5100}$$

$$I(\lambda 5003A) = 0.435\ I_{N1} + 12.4\ I_{\lambda 5100}$$

or

$$I(\lambda 5100A) = 0.518\ I_{N1} + 160.1\ I_{\lambda 5100}$$

$$-1.19 I(\lambda 5003A) = 0.518\ I_{N1} + 14.8\ I_{\lambda 5100}\ .$$

Then

$$145.3\ I_{\lambda 5100} = I(\lambda 5100A) - 1.19\ I(\lambda 5003A)$$

$$= 5.16 \times 10^{-3} - 2.74 \times 10^{-3},$$

and

$$I_{\lambda 5100} = 1.66 \times 10^{-5} \text{ ergs/cm}^2\text{/sec/ster/A.}$$

Substituting this value in equation (5.3), and rearranging,

$$I_{N1} = 2.3\ I(\lambda 5003A) - 28.5\ I_{\lambda 5100}$$

$$= 5.30 \times 10^{-3} - 4.74 \times 10^{-4}$$

$$I_{N1} = 4.83 \times 10^{-3} \text{ ergs/cm}^2\text{/sec/ster},$$

as given in Table 5.1

LIST OF REFERENCES

Allen, C.W. 1963, Astrophysical Quantities, 2nd ed. (London: Athlone Press), pp. 122 and 245.

Aller, L.H. 1951, Ap.J., 113, 125.

———. 1954, Ap.J., 120, 401.

———. 1956, Gaseous Nebulae (New York: Wiley and Sons).

Aller, L.H. and Liller, W. 1959, Ap.J., 130, 45.

Baker, J.G. and Menzel, C.H. 1938, Ap.J., 88, 52.

Baldwin, J.E. 1953, Obs., 73, 155.

Berman, L. 1936, MNRAS, 96, 980.

Bertola, F. 1962, Ric.Sci., 32(1), 5.

Blaauw, A. and Morgan, W.W. 1953, Ap.J., 117, 256.

Boyce, P.B. 1963, A.J., 66, 274, and private communication.

Burbidge, E.M. and Burbidge, G.R. 1962, Ap.J., 135, 694.

Burbidge, G.R., Gould, R.F. and Pottasch, S.R. 1963, Ap.J., 138, 945.

Campbell, W.W. and Moore, J.H. 1918, Publ.Lick Obs., 13, 77.

Capriotti, E.R. and Daub, C.T. 1960, Ap.J., 132, 667.

Code, A.D. 1960, Stellar Atmospheres, ed. J.L. Greenstein (Chicago: Univ. of Chicago Press), p.82.

Collins II, G.W.,Daub, C.T. and O'Dell, C.R. 1961, Ap.J., 133, 471.

Dufay, J. 1957, Galactic Nebulae and Interstellar Matter (New York: Philosophical Library), p.84.

Faulkner, D. 1962, Mt. Stromlo Obs., private communication.

Greenstein, J.L. 1946, Ap.J., 104, 414.

Greenstein, J.L. and Page, T.L. 1951, Ap.J., 114, 407.

Haddock, F.T., Mayer, C.H. and Sloanaker, R.M. 1954, Ap.J., 119, 456.

Hall, J.S. 1951, A.J., 56, 40.

Herrick, S. Jr. 1935, Lick Obs. Bull., 17, 85.

Hubble, E. 1922, Ap.J., 56, 400.

Johnson, H.L. and Morgan, W.W. 1951, Ap.J., 114, 522.

———————————. 1953, Ap.J., 117, 313.

Mathis, J.S. 1957, Ap.J., 125, 328.

Menon, T.K. 1958, Ap.J., 127, 28.

———. 1961, Pub. Nat. Radio Astr., 1,1.

Menzel, D.H. 1937, Ap.J., 85, 330.

Menzel, D.H. and Baker, J.G. 1937, Ap.J., 86, 70.

Menzel, D.H., Aller, L.H. and Hebb, M.H. 1941, Ap.J., 93, 230.

Minnaert, M. 1953, The Sun (Chicago: Univ. of Chicago Press), p.92.

Osterbrock, D.E. 1962, Ap.J., 135, 95.

Osterbrock, D.E. and Flather, E. 1959, Ap.J., 129, 26.

Page, T.L. 1942, Ap.J., 96, 78.

Seaton, M.J. 1958, Rev. Mod. Phys., 30, 979.

———. 1959, M.N., 119, 90.

Spitzer, L. and Greenstein, J.L. 1951, Ap.J., 114, 407.

Stebbins, J. and Kron, G.E. 1957, Ap.J., 126, 266.

Wyse, A.B. 1942, Ap.J., 95, 356.

Zanstra, H. 1931a, Pub. Dominion Ap. Obs. Victoria, 4, 209.

———. 1931b, Zs.f.Ap., 2, 1.

LIST OF NAMES

LIST OF SUBJECTS